KR9600254

KAERI/TR-693/96

Technical Report

Finite Element Modelling for Thermal Analysis of Stud-to-Plate Laser Brazing for a Dissimilar Metal Joint

이종금속 스터드와 평판간 레이저 브레이징 접합부의
열해석을 위한 유한요소 모델링

Korea Atomic Energy Research Institute

KAERI/TR-693/96

Technical Report

Finite Element Modelling for Thermal Analysis of Stud-to-Plate Laser Brazing for a Dissimilar Metal Joint

이종금속 스터드와 평판간 레이저 브레이징 접합부의 열해석을 위한 유한요소 모델링

Korea Atomic Energy Research Institute

제 출 문

한국원자력연구소장 귀하

본 보고서를 "이종금속 스터드와 평판간 레이저 브레이징 접합부의 열해석을 위한 유한요소 모델링" 보고서로 제출합니다.

1996년 6월

연구기관명 : 한국원자력연구소

참여연구원

주 저 자 : 박준수(계통기계분야)

공동저자 : 김종민(계통기계분야)

책임감수위원 : 김동훈

감수위원 : 김종인

Summary

A finite element model was developed for the thermal analysis of a stud-to-plate laser brazing, while the model was based upon a real-time observation of the filler metal motion. The finite element program ABAQUS, together with a few user subroutines, was employed to perform the numerical approximation and the transient temperature fields were analysed by using a three-dimensional model. The brazing materials used were AISI 304 stainless steel stud and aluminum plate Al 5052, and the brazing alloy 88Al-12Si was used as filler metal. The surface tension driven motion of the filler metal during the brazing process, including its wetting and spreading, was incorporated in the FEM modelling for defining the solution domain and boundary conditions. The numerical results showed a fairly good agreement with the experimental ones which were determined by using the infrared and thermocouple measurements.

LIST OF CONTENTS

LIST OF FIGURES

1. Introduction

Rivetting has been widely utilized in industries for joining small-sized stainless steel studs onto aluminium plate, while the industries have sought a better technology to improve the productivity of the stud-to-plate joining process. Laser brazing is considered as a potential candidate for this, and it offers advantages over conventional brazing processes because of its capability to produce a joint locally without heating the entire part or component to the flow temperature of the brazing filler metal. High degree of control for thermal energy input including the intensity, spot size, duration, and ability to be located or positioned precisely, is another merit of laser beams, in particular, for small or miniature parts joining(1 - 4).

The thermal behaviours of the workpiece during laser brazing is significantly different from the conventional methods, e.g. induction, resistance, furnace or torch brazing. The rates of heating and the differential thermal gradients are important to achieve a quality joint of dissimilar metal combination. The effects on the dimensional stability, distortion, and metallurgical structure of the brazed joint must be considered. In case of aluminium to stainless steel brazing, the temperature gradient produced by laser heating is high because of the great difference in their thermal properties, and this causes the filler metal to flow in undesired directions and imposes difficulties to control the filler metal penetration into the brazing gap. When the difference in melting point between the braze alloy and base metal is narrow, tight control of the brazing temperature is required and the heating cycle must be short to minimize the thermal effect on the base metal as well as to minimize the thermal distortion of the joint.

In the past decades, numerous studies on laser material processing have been performed using analytical or numerical approaches, while most of the studies were concentrated on the laser cutting, welding or surface treatment but rarely on laser brazing(5 - 11). In this study, a mathematical model was developed for

the calculation of heat transfer in stud-to-plate laser brazing, while the model was based on the experimental observation of the filler metal behaviour in the brazing. For the thermal analysis of small part joining process, experimental approaches are sometimes not practical because of measurement difficulties and it will be beneficial to employ a numerical approach using the computer simulation. Two studies have been conducted for the development of the laser brazing process to join stainless steel stud onto aluminium plate, which included two-dimensional finite element modelling for thermal analysis of the brazing process and the process monitoring technologies(12, 13).

2. Stud-to-Plate Laser Brazing

A schematic diagram of stud to plate laser brazing is shown in Fig. 1. The workpiece consists of 3mm diameter stainless steel stud and 1.2mm thick aluminium plate. Using a jig, an annular gap of 0.2mm is provided initially between the joining parts at the centre of the plate. A ring-shaped filler metal is pre-placed on the plate around the periphery of the stud. Considering the shape of filler metal and the geometry of joint, the cw CO_2 laser beam of a pseudo-TM_{01}^* mode was chosen as heat source. The materials used were Al 5052 aluminium and AISI 304 stainless steel, and the aluminium alloy 88Al-12Si was selected for the filler metal. The brazing is done in the atmosphere with aid of a brazing flux, and neither the pre-braze nor post-braze heating cycle was applied to control the thermal history of the joint. The studs to be joined with the plate function as guide posts or shafts for rollers, and major quality factors are the perpendicularity of stud to the plate and the joint strength.

During the brazing cycle a doughnut-shaped laser beam strikes the joint area and heats the workpiece locally in the size of 7.5 mm diameter. With build-up of heat, the brazing flux melts and covers over the beam impingement area and then the filler metal starts to melt at the initial position. The molten filler metal forms instantly a small drop being slightly deformed by the gravity. Once melted at the periphery of the stud, the filler metal drop moves in a few tenth seconds towards the centre of the joint, the highest temperature region, changing its free surface depending upon the wetting angles among the phases involved. Wetting of the filler metal is retarded untill the oxide film has been removed from the workpiece surface by the action of flux. After the filler metal re-locates at the centre, the filler metal starts to wet the workpiece and the heating cycle continues until the filler penetrates into the gap entailing a bead on the plate. The filler metal motion during the stud-to-plate laser brazing is more detailed in the author's study, including a real-time observation of the filler metal by using a high speed motion analyser(14).

As a result of extensive tests that were performed on various joint geometries and types of the filler metal, the current joint configuration and filler metal were chosen as a suitable condition(12, 13). The volume of filler metal in the conventional brazing is controlled by the size of the braze gap, but some attempts to reduce further the volume of filler metal for the laser brazing studied here have failed. All other joint designs which have been tested without the brazing bead on the top of joint were also not successful. The reason for this is probably owing to the highly localized laser heating and the dissimilar material combination of a large difference in the thermal properties.

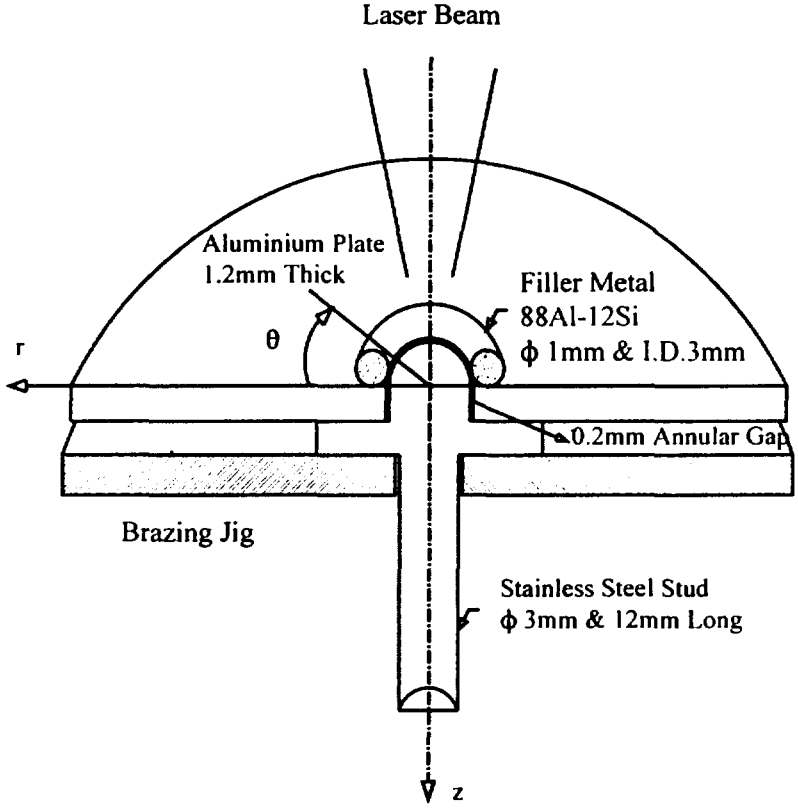

Fig. 1: Schematic Diagram of the Stud-to-Plate Laser Brazing

3. Solution Strategy and Analysis Method

The mathematical model of the heat transfer in laser brazing studied here is the one in which the temperature fields is strongly affected by the surface tension driven filler metal flow. The prime difficulty involved is to treat the dynamic behaviour of the filler metal in the analysis without penalty of reasonable accuracy and economy. Therefore, particular attention must be paid to simulate the filler metal movement when using the finite element method(FEM) for the thermal analysis of the brazing.

The filler metal movement in the stud-to-plate laser brazing is driven by a non-uniform temperature field, which is resulted from the localized laser heating of the workpiece of dissimilar materials. During the stud-to-plate laser brazing, the filler metal moves on the workpiece surface before the filler metal penetrates into the brazing gap and this affects considerably the energy absorptance of incident beam and the transient temperature fields in the workpieces. When temperature or composition gradients are present along the surface of liquid, a surface energy gradient exists and this gives rise to advance of the droplet triple point line to the higher temperature region(15, 16). The variation of surface energy with temperature and chemical potentials can be formulated by the Gibbs-Duhem equation(17). The spreading of the filler metal is governed by the surface kinetics and the motion of the triple point line. For non-interacting liquid-solid systems, the formulation of spreading kinetics is known by the equations of the capillary driving force and the viscous resisting force(18).

Ideally, a fully conjugate solution for heat conduction with the filler metal flow must be employed to precisely predict the temperature field of brazements. This presumes a finite element formulation of the filler metal behaviour which includes the dynamics of wetting and spreading during brazing. Without conjugate solutions of the heat conduction and filler metal flow, the analysis must be carried out for an infinitesimal length of time and the element meshes

for re-located filler metal and the corresponding boundary conditions must be defined before performing the analysis for another infinitesimal time step. From a practical point of view, however, the infinitesimal time step analysis is impossible and an approximate solution on the level of finite time and the discrete motion of filler metal has to be adopted. Instead of rigorous treatment of the dynamics of the filler metal motion, an approximate solution of thermal behaviour of the brazed joint was implemented using a finite element analysis. The definition of solution domain and boundary conditions for the molten filler metal were based on the results of experimental observation, and the motion of filler metal was divided into a few discrete steps in which the free surface formation and thermal contact condition of the filler metal were assumed to be unaltered.

Due to the axisymmetricity of the brazed joint, the temperature fields can be analysed by using a two-dimensional model(12). For the purpose of the process design improvement which is underway, a three-dimensional model is required to investigate the effects of beam offset from the centre line of the joint, and of blanks, cuts or edges in the plate. Except for the treatment of the motion of the molten filler metal, most of the FEM modelling techniques developed so far in the area of welding mechanics can be utilized for the thermal analysis of the laser brazing process (19 - 23).

4. Heat Transfer Analysis

4.1 Governing Equation and Boundary Conditions

Heat transfer problem of laser processing can be solved by applying the heat conduction theory, and the thermal and mechanical aspects of the problem can be decoupled without imposing any significant penalty of calculation accuracy. The assumptions for this are that the dimensional changes during brazing are insignificant and that the mechanical work done is negligible compared to the thermal energy changes. Thermal energy changes due to the chemical reactions and evaporation of material occurring during brazing were not considered.

The energy equation of the problem without any internal heat generation is:

$$\rho C_p \frac{\partial T}{\partial t} = \underline{\nabla}(k\underline{\nabla}T) \qquad [1]$$

Boundary conditions of the heat flux at surfaces by the Fourier equation:

$$q'' = -k\underline{\nabla}T \qquad [2]$$

$$\int\int_S K\frac{\partial T}{\partial n} = -\int\int_S A(T)I_0 dS + \sigma\int\int_S \varepsilon(T)(T^4 - T_0^4)dS + P_c \qquad [3]$$

where,

$T(r,\theta,z,t)$ = temperature — $K(T)$ = thermal conductivity

P_c = heat loss by convection — $\varepsilon(T)$ = hemispherical total emissivity

n = surface normal — $A(t)$ = absorptivity at laser wavelength

I_0 = power density of incident laser radiation

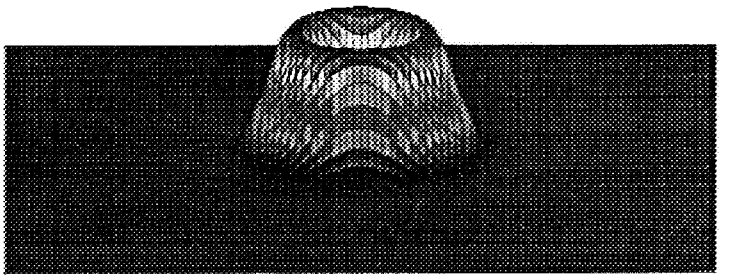

Fig. 2: Surface Contour of Heat Flux from the Optically Modulated TM_{01}^{*} Mode Beam

The heat flux q'' consists of the convective loss by the Newton's cooling law, the radiative dissipation by the Stefan-Boltzmann equation, and the specified heat flux at surfaces by incident laser beam. Initial condition for the transient analysis is $T(r,\theta,z,t) = T_0(r,\theta,z)$ at $t=0$, where T_0 is the initial temperature.

4.2 Heat Input Model

Heat input by the incident laser beam can be modelled by applying the heat flux at workpiece surfaces. For the doughnut shaped pseudo-TM_{01}^{*} mode which is optically modulated from the TM_{00} mode of the Gaussian energy distributuion, the expression of heat flux can be formulated as follows:

$$q''(r) = 1.89\frac{\alpha P}{\pi \bar{r}^2}\exp\left[-3\left(\frac{r-r_{sh}}{\bar{r}/2}\right)^2\right] \qquad [4]$$

In the above equation, r is the radial distance from the axis of impinging laser beam, $\bar{r}$ the characteristic radius (Gaussian beam radius) defined as the radial distance where the intensity of the beam falls to 5% of the central intensity, and Q the total heat transferred to the substrate. The α denotes the absorptivity of material and P the total incident laser power. In case of the centre-null distribution, r_{sh} is set equal to $\bar{r}/2$.

The equation of heat flux was formulated through the volume integration of beam energy by equalizing it to the total energy of TM_{00} mode generated in the beam oscillator. Graphical representation of the heat flux from the pseudo-TM_{01}^{*} mode is shown in Fig. 2. When defocussed with the beam diameter fixed, the shift distance r_{sh} is smaller than the characteristic beam radius $\bar{r}/2$, and a centre-fluxed distribution is obtained instead of the centre-null one.

4.3 Material Thermal Properties

The materials used were aluminium Al 5052-H34 plate and AISI type 304 stainless steel stud. Braze alloy 88Al-12Si was used as the filler metal, which has the eutectic point of 12.7wt% silicon. The thermal properties of materials are assumed isotropic and homogeneous but are depending upon temperature. Temperature dependent thermal properties assumed for the materials are shown in Figs. 3 and 4, respectively(24 - 26). Latent heat of fusion used for Al 5052 was 408 J/g to be released or absorbed over the temperature range from T_S=607°C to T_L=649°C. Properties of the braze alloy were not available, and the same values as those of Al 5052 were assumed except that the latent heat in the temperature range from T_S=577°C to T_L=582°C was assumed considering the contribution of each alloy constituent. To simulate the stirring action inside the molten filler metal, an effective conductivity k_{eff} which was increased about two times was used for the filler metal above its melting point.

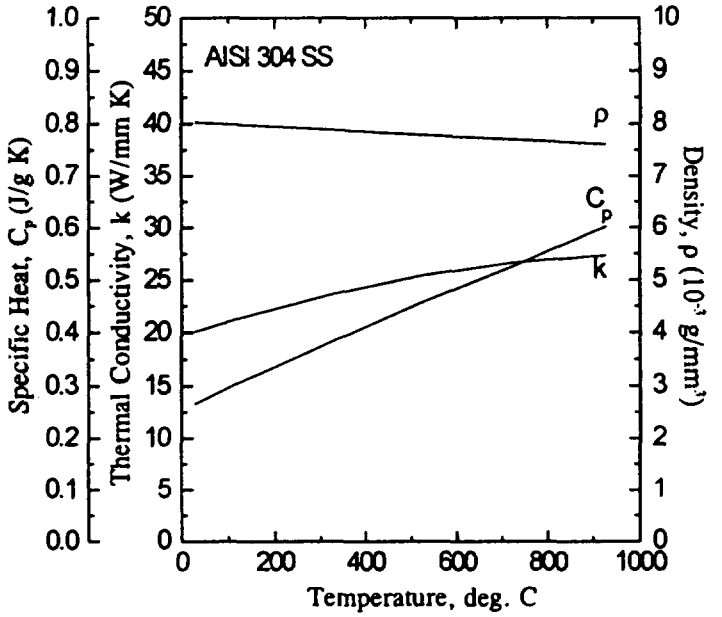

Fig. 3: Thermal Properties Used for AISI 304 Stainless Steel

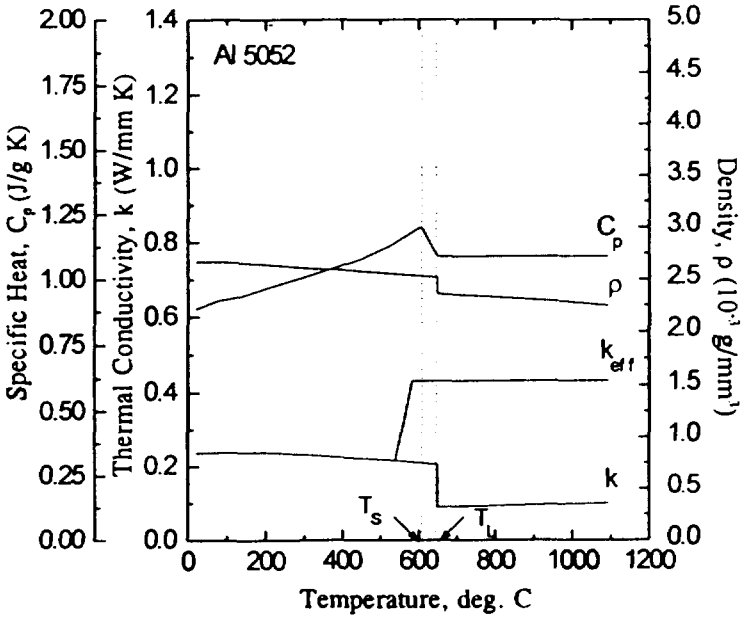

Fig. 4: Thermal Properties Used for Aluminium 5052

4.4 Surface Heat Losses

During laser brazing using the flux in the atmosphere, heat losses from workpiece surfaces are through natural convection, radiation, and evaporation of molten metal or flux. Convective and radiative heat losses only were applied for this study. The convective heat loss is represented by Newton's cooling law $q''= h(T-T_a)$, and the film coefficient used was h=10W/m^{2}K(20 - 22). The radiative heat losses were accounted for all the surfaces by using the Stefan Boltzmann equation $q''= \bar{\varepsilon}\sigma(T^4-T_a^4)$, and the emissivity values of 0.25 for stainless steel and 0.09 for aluminium were assumed, respectively(19, 20).

4.5 Absorptivity of Materials

The value of absorptivities when used for the thermal analysis of laser heating has a profound effect on the results. The absorptivity properties of metal substrates of beam energy varies interactively upon the surface roughness, temperature and the wave length of the incident beam. Aluminium is a highly reflective material and its absorptivity of infrared energy at 10.6 μm ranges from the value less than 10% at room temperature to between 40% and 50% at the melting point, and goes as high as 90% at its vaporization point (27). Same value of absorptivity as Al 5052 was used for the alloy 88Al-12Si. The absorptivity of type 304 stainless steel is less dependent upon the temperature variation, and shows a rather uniform value of about 10% (28, 29). For convenience, a constant value of absorptivity was assumed for a range of temperature.

4.6 Effect of Braze Flux

When using the braze flux, the surface of workpieces is covered with thin film of the molten flux where the chemical reactions with metal oxides and mass transfer through evaporation occur. Coverage of the workpiece surface with the flux film was found to significantly increase the absorption of beam energy.

Based on the previous study on the laser heating for the same materials as used here, an effective absorptivity of 35% was applied for the materials when covered with molten flux(12). The effect of material evaporation losses has been reflected in the determination of the effective absorptivity, and the energy change due to chemical reactions is negligibly small. Thermal blanketing for the workpieces with the flux film is also an effect that has to be considered for such a fast laser heating. To simply account for this effect, the surface temperature of the workpiece when covered by the molten flux was assumed to be at an average working temperature of the flux.

5. Finite Element Modelling

The transient temperature fields of the stud to plate joint produced by laser brazing were analysed by using a three-dimensional finite element model. The finite element program ABAQUS, together with a few user subroutines, was employed to obtain the numerical results. ABAQUS employs a front wave solver to solve the equation system by using Gaussian elimination in an efficient manner. More information of solution techniques is described in ABAQUS users manuals(30).

The FEM model idealized for each step of the thermal analysis is shown in Figs. 5a, 5b and 5c, respectively. Based on the results of experimental observation, three sets of domain for the filler metal were defined for which the free surface of the filler metal was assumed to be unchanged for a certain period of time. For each step of analysis, the solution model is changed using Model Change Option as provided by ABAQUS. Each model change requires an intermediate step for application of the thermal boundary conditions, which is followed by the main step for calculating the temperature fields. Definition of the model and the corresponding boundary conditions are described below.

The first analysis model in Fig. 5a corresponds to the time period during which the filler metal heats up at the initial position until its movement to the central region of joint. During this period, the interfacial heat transfer between the solid filler metal and the plate was assumed to be adiabatic, considering the inadequate thermal contact between two solids before the complete melt down of filler metal. This assumption sacrifices the accuracy of simulations from the time of filler metal melt-down to the completion of its re-location at the joint centre. The second model of Fig. 5b, the filler metal drop has moved to the centre of joint where it wets over the whole surface of stud and contacts by gravity on the edge of the plate near the gap. It was assumed that the filler metal drop formed late in the first step re-locates instantly to the centre of joint. During the second step the filler metal thermally connects the parts, and this

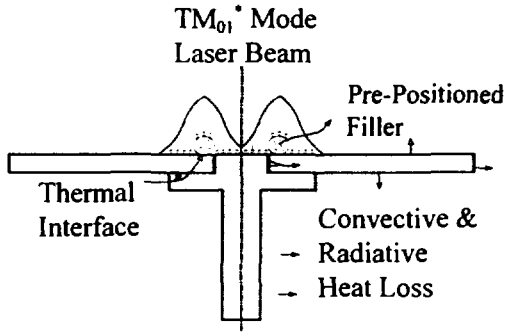

(a)

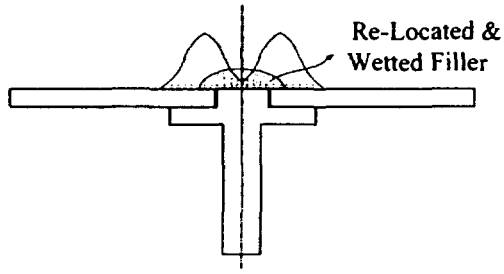

(b)

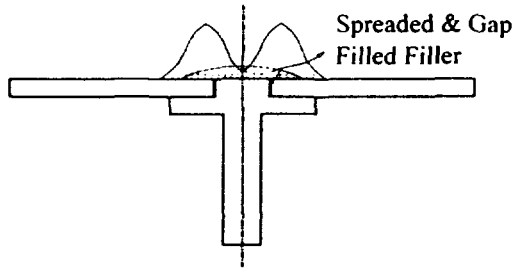

(c)

Fig. 5: FEM Solution Domains: a) The First Step Analysis for Pre-Positioned Filler Metal; b) The Second Step Analysis for The Re-located and Wetted Filler Metal; c) The Third Step Analysis for the Spreaded and Gap Penetrated Filler Metal

speeds up the heating of the plate near the gap. In the third model of Fig. 5c, the filler metal has spreaded over the workpiece surface to the size of brazing bead, and the thermal contact at the interface between the filler metal and stud or plate was assumed to be perfect. This step starts at the time when the area near the edge of the wetted filler metal is heated up sufficiently for the filler metal to spread. At the later stage of this step, the filler metal penetrates into the brazing gap when the gap boundary is heated up to the flow point of the filler. Then, within a few tenth seconds, the beam is shut off and the brazement begins to cool. The computation scheme using ABAQUS is shown in Fig. 6.

A three dimensional model with eight-noded isoparametric elements is shown in Fig. 7 for the solution domain applied for the first step analysis. The linear elements which utilizes a trapezoidal numerical integration scheme have been used over the whole solution domain, so that the discontinuous temperature gradient at the solid/liquid interface can be simulated smoothly and the adverse effects of the latent heat involved in the phase change can be minimized(22, 30). When implementing a transient heat transfer analysis, an appropriate time-stepping scheme is required to ensure a convergence and accuracy. In consideration of fast heating and cooling in laser brazing, relatively short time increment and less severe convergence criteria were used. Total number of elements was 1568, and the CPU time for a brazing cycle of ten seconds was 1912.4 seconds.

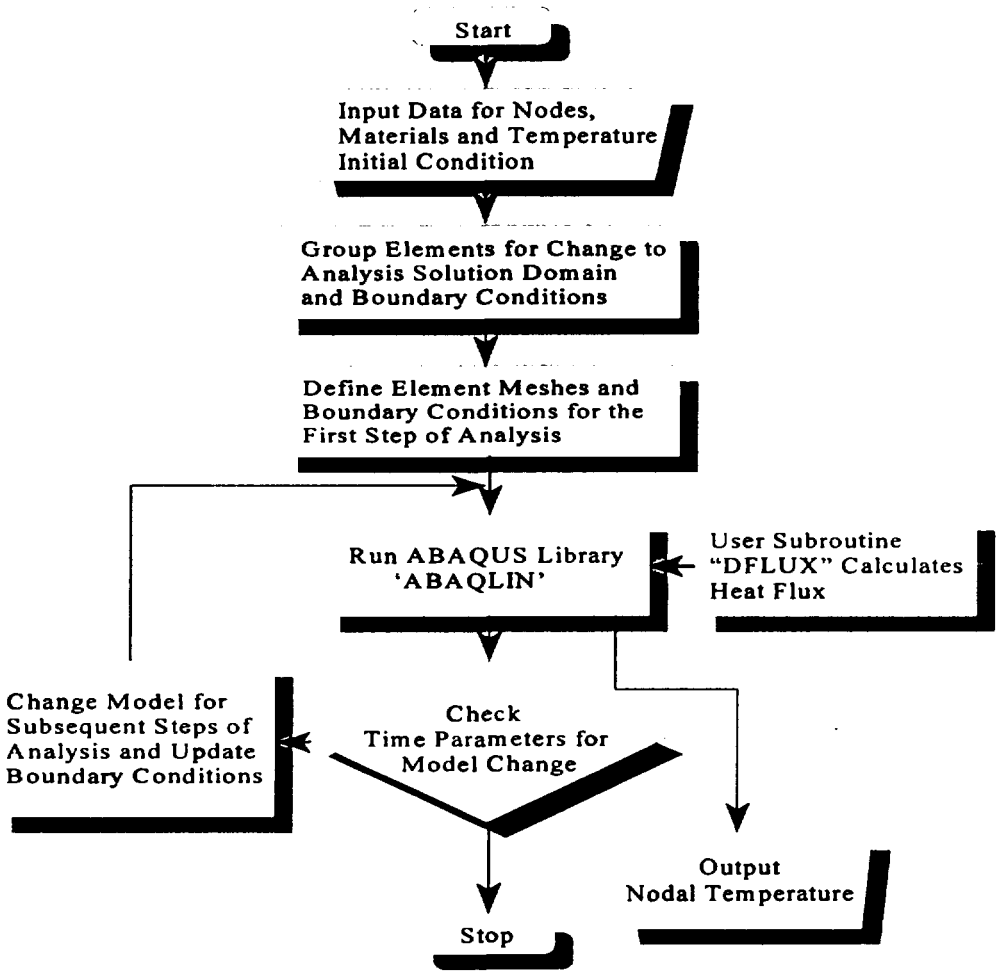

Fig. 6: Flow Chart for the Thermal Analysis of Stud-to-Plate Laser Brazing Process

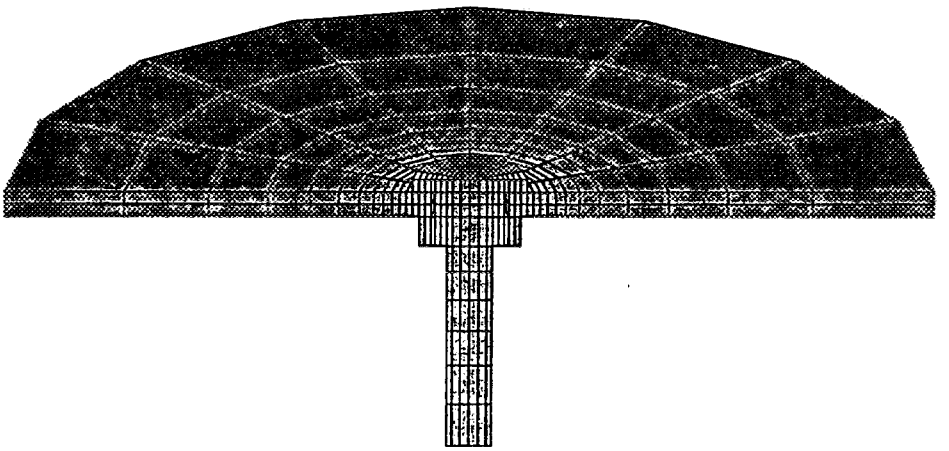

Fig. 7: Section of the 3D FEM Model for the Thermal Analysis of Stud-to-Plate Laser Brazing

6. Experiments

Experiments were designed to verify the FEM model of the brazing as well as to validate the boundary conditions assumed for the thermal analysis. An experimental set-up for the CO_2 laser brazing is shown in Fig. 8. The laser brazing system consists of a power supply, laser delivery head, HeNe probe laser, CNC controller, X-Y table and computer. The beam oscillator is capable of the maximum output power 700W and generates a continuous beam of wave length 10.6 μm in the TM_{00} mode. Through the optical modulation using the focussing lens and axicon lens, this mode was transformed into a pseudo-TM_{01}^* of a doughnut-shaped beam flux. The beam delivery head was fixed, and the workpiece alignment was facilitated by the X-Y table and the probe laser. A side blower using the compressed air was also used to protect the optical parts from contamination.

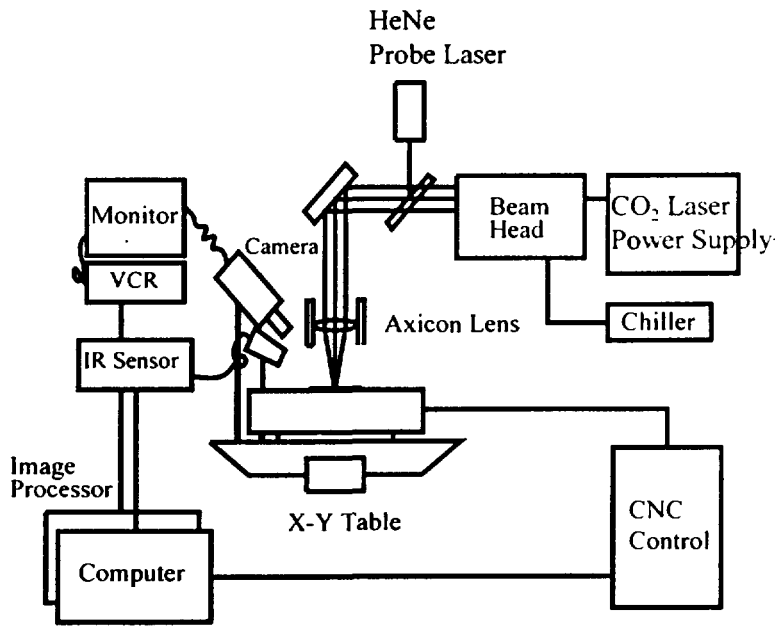

Fig. 8: Experimental Setup for Tests of the Stud-to-Plate Laser Brazing

The brazing materials were surface prepared by pickling for AISI 304 stainless steel studs(10% cold nitric acid, 0.25% hydrofluoric acid for 5 mins.), and by vapour cleaning for aluminium AL 5052 plate and filler metal. After a series of pre-experiments on various combinations of the process parameters, the beam-on-time for brazing was set by 3 seconds at the power of 550W for the ring- shaped filler metal of ϕ 1mm and 5mm O.D.

Temperature measurements were done by using an non-contact infrared sensor(IR) for the laser irradiated spot of about 4mm diameter, which had been calibrated by employing the numerical simulation and thermocouple measurements (12). The measurement for the stud was done by a thermocouple attached below the bottom of brazing gap.

7. Results and Discussions

The isotherms in the brazed area are shown in Figs. 9 and10, and the curves were drawn for the laser output of 550W and the total beam-on-time of 3.0 sec. The curves depict the pattern of heat flow at the beam-on-time of 0.896 sec. and 2.5 sec., respectively. It is noticed that heat flow in the base materials is mainly from the molten filler metal. The heat of the filler metal increased effectively the temperature of base metals in the joint area. The temperature contour as shown in Fig. 9 was obtained from the second step analysis, where the molten filler metal has moved to the centre of joint. At this time, the heat was highly localized around the filler metal at the centre of joint, but the gap boundary on the both sides of stud and plate had not been heated sufficiently for the filler metal to flow. The contour as shown in Fig. 10 was obtained from the third step analysis where the filler metal have spreaded to the final size of the bead. It shows the temperature contour 0.04sec. after the filler metal penetration into the gap. Before this, both sides of the brazing gap boundary were heated to the flow temperature of the filler metal and the filler metal was penetrated into the gap. The temperature gradient in the joint area was decreased due to the metallurgical connection between the parts.

Figure 11 plots the temperature history of the joint area and shows a fairly good agreement between the computation results and experimental measurements. The computed results of the filler metal temperature shows a faster heating and cool down at the initial stage than the infrared measurement. This was probably owing to the boundary conditions that the adiabatic contact between the solid filler metal and the plate was assumed in the first step analysis, while the perfect contact among the molten filler metal and the stud and plate was assumed in the second step. The simulated filler metal temperature was in a fairly good agreement with the measurement, after the filler metal relocated at the centre of the joint. The computed results of the stud temperature at z=3.0mm shows a faster heating and higher peak temperature than the thermocouple measurement.

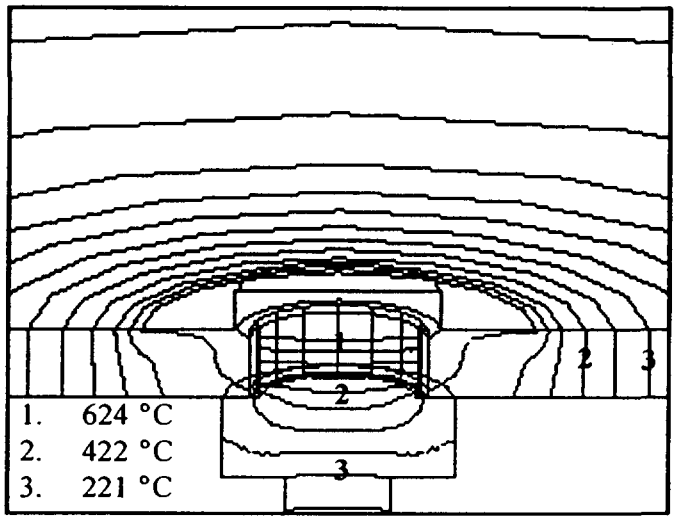

Fig. 9: Calculated Temperature Contours of the Brazing Joint Area at Beam-on-Time of 0.896 Sec.

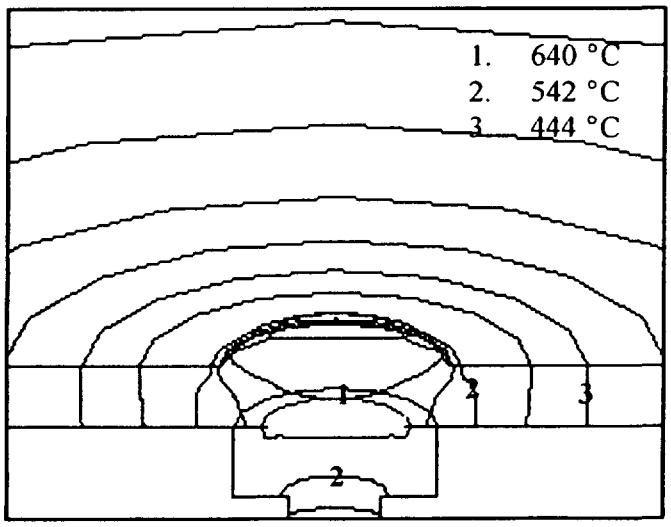

Fig. 10: Calculated Temperature Contours of the Brazing Joint Area at Beam-on-Time of 2.50 Sec.

Due to the highly localized heating by laser beam, the thermal behaviour of the brazing joint is significantly different from the conventional heating and this necessitated the high speed motion analysis of the filler metal movement for the definition of the FEM solution domain and boundary conditions. The free surface formation of the molten filler metal during brazing is driven by the surface tension among the phases involved and the temperature field, and the movement of the filler metal is due to a large temperature gradient established in the brazing area of the dissimilar metals, i.e. aluminium and stainless steel with a great difference in the thermal diffusivity.

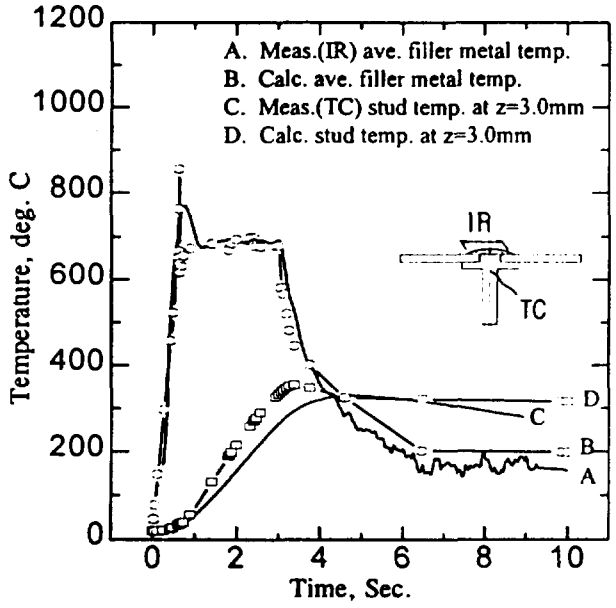

Fig. 11: Calculated Temperature and Comparison with the Infrared and Thermocouple Measurements

8. Concluding Remarks

From the results of FEM modelling and the experiments for the heat transfer analysis of the stud-to-plate laser brazing, the following conclusions may be drawn:

1) Without a conjugate analysis of the heat conduction and filler metal flow, the FEM model is capable of predicting the temperature history of the stud-to-plate laser brazing joint in a reasonable accuracy and the results can be used further for analysing the distortion or residual stresses of the brazing joint.

2) The filler metal movement occuring in the stud-to-plate laser brazing is due to the highly localized heating, and this affects strongly the transient temperature field of the dissimilar metal joint. Therefore, the effect of the filler metal movement must be considered in defining the solution domain and boundary conditions for the thermal analysis of the brazing.

3) The joining of stainless steel stud to aluminium plate by the laser brazing is a new technology which is still under development program. The three-dimensional FEM model developed can be utilized further to investigate the three-dimensional effects due to the beam offsets, material cuts or blanks and the joint misalignments. This study will provide the useful data such as to optimize the dissimilar metal joining.

References

1. C. E. Witherell and T. J. Ramos: 'Laser Brazing', Welding Journal, Vol 59, p267s, 1980.
2. Brazing Manual, 3rd ed., American Welding Society, Miami, 1976.
3. T. A. Jones and C. E. Albright: 'Laser Beam Brazing of Small Diameter Copper Wires to Laminated Copper Circuit Boards', Welding Journal, Vol 63, p34, 1984.
4. C. E. Witherell: 'Laser Micro-Brazing to Join Small Parts', Laser Focuses, p73-80, Nov 1981.
5. Y. Arata and I. Miyamoto: 'Some Fundamental Properties of High Power Laser Beam as a Heat Source (Reports 1, 2 and 3)', Trans. Japan Welding Society, Vol 3, No 1, p143, Apr 1972.
6. M. Sparks: 'Theory of Laser Heating of Solids: Metals', J. Applied Physics, Vol 47, No 3, p837, Mar 1976.
7. H. E. Cline and T. R. Anthony: 'Heating Treating and Melting Material with a Scanning Laser or Electron Beam', J. Applied Physics, Vol 48, No 9, p3895, Sep 1977.
8. M. Lax: 'Temperature Rise Induces by a Laser Beam', J. Applied Physics, Vol 48, No 9, p3919, Sep 1977.
9. J. E. Moody and R. H. Hendel: 'Temperature Profiles Induced by a Scanning cw Laser Beam', J. Applied Physics, Vol 53(6), p4364, Jun 1982.
10. J. Mazumder and W. M. Steen: 'Heat Transfer Model for CW Laser Material Processing', J. Applied Physics, Vol 51(2), p941, Feb 1980.
11. Y.-S. Yang: 'A Study on the Residual Stress in Thermal Processing by the Arc and Laser Beam', Ph.D dissertation, Korea Advanced Institute of Science and Technology, 1991.
12. M.-K. Jeon: 'A Study on Analysis of Heat Flow and Development of Temperature Measuring System in Laser Brazing', M.SC Thesis, Korea Advanced Institute of Science and Technology, 1995.
13. W.-S. Chang: 'A study on Three Dimensional Heat Transfer Analysis and Process Monitoring of Pin to Hole Joining', M.SC Thesis, Korea Advanced

Institute of Science and Technology, 1996.

14. J.-S. Park, W.-S. Chang, H.-J. Chang and S.-J. Na, 'A Three-Dimensional Finite Element Analysis of Thermal Behaviour in Stud-to-Plate Laser Brazing', Proce Int. Conf. In Computer Technology in Welding, Lanaken, Belgium, 9-12, Jun 1996.
15. F. G. Yost, F. M. Hosking and D. R. Frear: 'The Mechanics of Solder Alloy Wetting and Spreading', Van Nostrand Reinhold, New York, p196, 1993.
16. Lau, W.Y., ans C. M. Burns: Surface Science, 30:467, 1972.
17. Levinson, P. Et al, 'Rev. Phys. Appl.' 23:1009, 1988.
18. deGennes, P. G., 'Rev. Mod. Phys.' 57:827, 1985.
19. Newman, Sandra Zeller: 'FEM Model of 3D Transient Temperature and Stress Fields in Welded Plates', Ph.D Dissertation, Carnegie-Mellon University, 1986.
20. P. Tekriwal, M. Stitt and J. Mazumder: 'Finite Element Modelling of Heat Transfer for Gas Tungsten Arc Welding', Metal Construction, p599R, Oct 1987.
21. C. K. Leung, R. J. Pick and D. H. B. Mok: 'Finite Element Modelling of a Single Pass Weld', Welding Research Council Bulletin, No 356, p1, Aug 1990.
22. P. Tekriwal and J. Mazumder: 'Finite Element Analysis of Three-Dimensional Transient Heat Transfer in GMA Welding', Welding Research Supplement, Welding Journal, p153s, Jul 1988.
23. A. Paul and T. DebRoy: 'Heat Transfer and Fluid Flow in Laser Melted Weld Pools', Proce Int. Conf on Trends in Welding Research, Gatlinburg, Tennessee, U.S., p29, May 1986.
24. E. F. Rybicki et al: 'A Finite Element Model for Residual Stresses and Deflections in Girth-Butt Welded Pipes', Trans. ASME Vol 100, p256, Aug 1978.
25. B. P. Bardes: 'Metals Handbook', 9th ed. Vol 2, American Society of Metals, 1978.
26. Y. S. Touloukian: 'Thermophysical Properties of High Temperature Solid Materials', Macmillan, New York, Thermophysical Properties Research

Centre, Purdue Univ., 1967.

27. Simon L. Engel: 'Kilowatt Welding with a Laser', Laser Focuses, p44, Feb 1976.
28. G. Sten: 'Absorptivity of cw CO_2, CO and YAG-Laser Beam by Different Metal Alloys', Proce ECLAT '90 Conf, Erlangen, Germany, p25, Sep. 1990.
29. T.-H. Kim et al: 'Absorptance of CO_2 Laser Beam on Stainless Steel and Carbon Steel by Numerical Method', Proce LAMP '92 Conf, Nagaoka, Japan, p287, Jun 1992.
30. Hibbit, Karlsson & Sorensen, Inc: ABAQUS Manuals,Version 5.3, Providence, RI, 1993.

Appendix

Program List

```
*HEADING
3D Thermal Analysis for Stud-To-Plate Laser Brazing Process
TM01* mode;fn=lbrzt1s. for Al 5052 and 3mm ID filler
********************************************************************************
*PREPRINT,ECHO=NO,HISTORY=NO,MODEL=NO
********** Node generation for pin **********
*NODE,SYSTEM=C
99, 0., 0., 12.
699, 0., 0., 1.8
999, 0., 0., 0.0
*NODE, SYSTEM=C, NSET=PN01
1, 0.4, 0.0, 12.
2, 0.5, 45.0, 12.
3, 0.75, 0.0, 12.
4, 0.72, 27.5, 12.
5, 0.83, 45., 12.
6, 0.72, 62.5, 12.
*NCOPY, CHANGE NUMBER=10, OLD SET=PN01, SHIFT, NEW SET=PN021,
MULTIPLE=1
0., 0., 0.0
0., 0., -100., 0., 0., 100., 90.
*NCOPY, CHANGE NUMBER=10, OLD SET=PN021, SHIFT, NEW SET=PN022,
MULTIPLE=1
0., 0., 0.0
0., 0., -100., 0., 0., 100., 90.
*NCOPY, CHANGE NUMBER=10, OLD SET=PN022, SHIFT, NEW SET=PN023,
MULTIPLE=1
0., 0., 0.0
0., 0., -100., 0., 0., 100., 90.
*NODE, SYSTEM=C
41, 1.0, 0., 12.
49, 1.0, 180., 12.
57, 1.0, 0., 12.
*NODE, SYSTEM=C
81, 1.5, 0., 12.
89, 1.5, 180., 12.
97, 1.5, 0., 12.
*NGEN, LINE=C, NSET=PN03, SYSTEM=C
41, 49, 1, 99,,,, 0., 0., 100.
49, 57, 1, 99,,,, 0., 0., 100.
*NGEN, LINE=C, NSET=PN04, SYSTEM=C
81, 89, 1, 99,,,, 0., 0., 100.
```

```
89, 97, 1, 99,,,, 0., 0., 100.
*NFILL, BIAS=1.1, NSET=PN34
PN03, PN04, 2, 20
*NSET, NSET=PN00
PN01, PN021, PN022, PN023, PN34, 99

*NCOPY, CHANGE NUMBER=600, OLD SET=PN00, SHIFT, NEW SET=PN60
0., 0., -9.4
0., 0., -100., 0., 0., 100., 0.
*NFILL, BIAS=1.1, NSET=PN060
PN00, PN60, 6, 100
*NCOPY, CHANGE NUMBER=700, OLD SET=PN00, SHIFT, NEW SET=PN70
0., 0., -10.8
0., 0., -100., 0., 0., 100., 0.
*NODE, SYSTEM=C
2601,1.7,0.,2.6
2609,1.7,180.,2.6
2616,1.7,-22.5,2.6
2661,2.5,0.,2.6
2669,2.5,180.,2.6
2676,2.5,-22.5,2.6
2701,1.7,0.,1.201
2709,1.7,180.,1.201
2716,1.7,-22.5,1.201
2761,2.5,0.,1.201
2769,2.5,180.,1.201
2776,2.5,-22.5,1.201
798,0.,0.,1.201
*NGEN, LINE=C, SYSTEM=C, NSET=PN61X
2601,2609,1,699,,,, 0., 0., 100.
2609,2616,1,699,,,, 0., 0., 100.
*NGEN, LINE=C, SYSTEM=C, NSET=PN62X
2661,2669,1,699,,,, 0., 0., 100.
2669,2676,1,699,,,, 0., 0., 100.
*NGEN, LINE=C, SYSTEM=C, NSET=PN71X
2701,2709,1,798,,,, 0., 0., 100.
2709,2716,1,798,,,, 0., 0., 100.
*NGEN, LINE=C, SYSTEM=C, NSET=PN72X
2761,2769,1,798,,,, 0., 0., 100.
2769,2776,1,798,,,, 0., 0., 100.
*NFILL,BIAS=0.95,NSET=PN612
PN61X,PN62X,3,20
*NFILL,BIAS=0.95,NSET=PN712
PN71X,PN72X,3,20
*NSET,NSET=PN67X
PN612,PN712,798
```

```
*NCOPY, CHANGE NUMBER=200, OLD SET=PN70, SHIFT, NEW SET=PN90
0., 0., -1.2
0., 0., -100., 0., 0., 100., 0.
*NFILL, BIAS=1., NSET=PN790
PN70, PN90, 2, 100
*NSET, NSET=PNALL
PN060, PN70, PN67X, PN790
*NSET, NSET=CP01, GEN
81, 681, 100
*NSET, NSET=CP02, GEN
97, 697, 100
*NSET, NSET=GPNS, GEN
781, 796
881, 896
981, 996
********** Node generation for plate **********
*NODE, SYSTEM=C
1001, 1.7, 0., 1.2
1009, 1.7, 180., 1.2
1017, 1.7, 0., 1.2
1061, 2.5, 0., 1.2
1069, 2.5, 180., 1.2
1077, 2.5, 0., 1.2
1141, 3.75, 0., 1.2
1149, 3.75, 180., 1.2
1157, 3.75, 0., 1.2
1301, 20., 0., 1.2
1309, 20., 180., 1.2
1317, 20., 0., 1.2
*NGEN, LINE=C, NSET=AN101, SYSTEM=C
1001, 1009, 1, 799,,,, 0., 0., 100.
1009, 1017, 1, 799,,,, 0., 0., 100.
*NGEN, LINE=C, NSET=AN102, SYSTEM=C
1061, 1069, 1, 799,,,, 0., 0., 100.
1069, 1077, 1, 799,,,, 0., 0., 100.
*NGEN, LINE=C, NSET=AN103, SYSTEM=C
1141, 1149, 1, 799,,,, 0., 0., 100.
1149, 1157, 1, 799,,,, 0., 0., 100.
*NGEN, LINE=C, NSET=AN104, SYSTEM=C
1301, 1309, 1, 799,,,, 0., 0., 100.
1309, 1317, 1, 799,,,, 0., 0., 100.
*NFILL, BIAS=0.95, NSET=AN120
AN101, AN102, 3, 20
*NFILL, BIAS=0.9, NSET=AN130
AN102, AN103, 4, 20
*NFILL, BIAS=0.7, NSET=AN140
```

```
AN103, AN104, 8, 20
*NSET, NSET=AN100
AN120, AN130, AN140
*NCOPY, CHANGE NUMBER=500, OLD SET=AN100, SHIFT, NEW SET=AN150
0., 0., -0.6
0., 0., -100., 0., 0., 100., 0.
*NCOPY, CHANGE NUMBER=1000, OLD SET=AN100, SHIFT, NEW SET=AN200
0., 0., -1.2
0., 0., -100., 0., 0., 100., 0.
*NSET, NSET=ANALL
AN100, AN150, AN200
*NSET, NSET=CA101, GEN
1021, 1301, 20
*NSET, NSET=CA102, GEN
1037, 1317, 20
*NSET, NSET=CA151, GEN
1521, 1801, 20
*NSET, NSET=CA152, GEN
1537, 1817, 20
*NSET, NSET=CA201, GEN
2061, 2301, 20
*NSET, NSET=CA202, GEN
2077, 2317, 20
*NSET, NSET=CA200, GEN
2001, 2301, 20
*NSET, NSET=GANS, GEN
1001, 1016
1501, 1516
2001, 2016
*NSET, NSET=AX901, GEN
2001, 2017
*NSET, NSET=AX902, GEN
2021, 2037
*NSET, NSET=AX903, GEN
2041, 2057
*NSET, NSET=AX904, GEN
2061, 2077
*NSET, NSET=AN901
AX901,AX902,AX903,AX904
********** Node generation for filler metal & its interface **********
** Filler metal before melting **
*NODE, SYSTEM=C
3099, 0., 0., -1.E-3
3299, 0., 0., -1.11784
3001, 1.5, 0., -1.E-3
3009, 1.5, 180., -1.E-3
```

```
3017, 1.5, 0., -1.E-3
3021, 1.7, 0., -1.E-3
3029, 1.7, 180., -1.E-3
3037, 1.7, 0., -1.E-3
3081, 2.5, 0., -1.E-3
3089, 2.5, 180., -1.E-3
3097, 2.5, 0., -1.E-3
*NGEN, LINE=C, NSET=FN301, SYSTEM=C
3001, 3009, 1, 3099,,,, 0., 0., 100.
3009, 3017, 1, 3099,,,, 0., 0., 100.
*NGEN, LINE=C, NSET=FN302, SYSTEM=C
3021, 3029, 1, 3099,,,, 0., 0., 100.
3029, 3037, 1, 3099,,,, 0., 0., 100.
*NGEN, LINE=C, NSET=FN306, SYSTEM=C
3081, 3089, 1, 3099,,,, 0., 0., 100.
3089, 3097, 1, 3099,,,, 0., 0., 100.
*NFILL, BIAS=0.95, NSET=FN300
FN302, FN306, 3, 20
*NSET, NSET=FN310
FN300, FN301
*NCOPY, CHANGE NUMBER=200, OLD SET=FN310, SHIFT, NEW SET=FN320
0., 0., -0.7856
0., 0., -100., 0., 0., 100., 0.
**0., 0., -0.89714
***NSET, NSET=FNALL
**FN310, FN320
*NSET, NSET=CF11
3001, 3021, 3041, 3061, 3081
*NSET, NSET=CF12
3017, 3037, 3057, 3077, 3097
*NSET, NSET=CF21
3201, 3221, 3241, 3261, 3281
*NSET, NSET=CF22
3217, 3237, 3257, 3277, 3297
**
*NODE, SYSTEM=C
3399, 0., 0., -1.E-3
3301, 1.5, 0., -1.E-3
3309, 1.5, 180., -1.E-3
3317, 1.5, 0., -1.E-3
3321, 1.7, 0., -1.E-3
3329, 1.7, 180., -1.E-3
3337, 1.7, 0., -1.E-3
3381, 2.5, 0., -1.E-3
3389, 2.5, 180., -1.E-3
3397, 2.5, 0., -1.E-3
```

```
*NGEN, LINE=C, NSET=XN301, SYSTEM=C
3301, 3309, 1, 3399,,,, 0., 0., 100.
3309, 3317, 1, 3399,,,, 0., 0., 100.
*NGEN, LINE=C, NSET=XN302, SYSTEM=C
3321, 3329, 1, 3399,,,, 0., 0., 100.
3329, 3337, 1, 3399,,,, 0., 0., 100.
*NGEN, LINE=C, NSET=XN306, SYSTEM=C
3381, 3389, 1, 3399,,,, 0., 0., 100.
3389, 3397, 1, 3399,,,, 0., 0., 100.
*NFILL, BIAS=0.95, NSET=XN300
XN302, XN306, 3, 20
*NSET,NSET=FBNDX,GEN
**3321,3336
**3341,3356
3361,3376
*NSET, NSET=XN310
XN300, XN300
*NSET, NSET=FNALL
FN310, FN320,XN310,3099,3299,3399
** Filler metal after melting upto the start of gap filling **
** Nodes for interim model change just after melting ***
*NCOPY, CHANGE NUMBER=3100, OLD SET=PN00, SHIFT, NEW SET=FBND1
0., 0., -12.528
0., 0., -100., 0., 0., 100., 0.
** Nodes for model change after melting: use two lares on plate ***
*NCOPY, CHANGE NUMBER=5000, OLD SET=PN00, SHIFT, NEW SET=PFN1C
0., 0., -12.0
0., 0., -100., 0., 0., 100., 0.
*NCOPY, CHANGE NUMBER=5500, OLD SET=PN00, SHIFT, NEW SET=PFN10
0., 0., -12.6694
0., 0., -100., 0., 0., 100., 0.
*NCOPY, CHANGE NUMBER=3100, OLD SET=AN901, SHIFT, NEW SET=AF91C
0., 0., 0.0
0., 0., -100., 0., 0., 100., 0.
*NCOPY, CHANGE NUMBER=3600, OLD SET=AN901, SHIFT, NEW SET=AFN91
0., 0., -0.6694
0., 0., -100., 0., 0., 100., 0.
*NSET, NSET=FBND2
PFN10, AFN91
**
** Filler metal after the gap filling with entail of bead .19376mm h**
*NCOPY, CHANGE NUMBER=6000, OLD SET=PN00, SHIFT, NEW SET=PFN2C
0., 0., -12.0
0., 0., -100., 0., 0., 100., 0.
*NCOPY, CHANGE NUMBER=6500, OLD SET=PN00, SHIFT, NEW SET=PFN20
0., 0., -12.5648
```

```
0., 0., -100., 0., 0., 100., 0.
*NCOPY, CHANGE NUMBER=4100, OLD SET=AN901, SHIFT, NEW SET=AFN2C
0., 0., 0.0
0., 0., -100., 0., 0., 100., 0.
*NCOPY, CHANGE NUMBER=4600, OLD SET=AX901, SHIFT, NEW SET=AFN21
0., 0., -0.4775
0., 0., -100., 0., 0., 100., 0.
*NCOPY, CHANGE NUMBER=4600, OLD SET=AX902, SHIFT, NEW SET=AFN22
0., 0., -0.3899
0., 0., -100., 0., 0., 100., 0.
*NCOPY, CHANGE NUMBER=4600, OLD SET=AX903, SHIFT, NEW SET=AFN23
0., 0., -0.3022
0., 0., -100., 0., 0., 100., 0.
*NSET, NSET=AFN92
AFN21, AFN22, AFN23
*NSET, NSET=FBND3
PFN20, AFN92
********** Node generation for model change of the gap **********
*NODE, SYSTEM=C
3441, 1.5, 0., 1.2
3449, 1.5, 180., 1.2
3457, 1.5, 0., 1.2
3461, 1.7, 0., 1.2
3469, 1.7, 180., 1.2
3477, 1.7, 0., 1.2
*NGEN, LINE=C, NSET=DN700, SYSTEM=C
3441, 3449, 1, 799,,,, 0., 0., 100.
3449, 3457, 1, 799,,,, 0., 0., 100.
3461, 3469, 1, 799,,,, 0., 0., 100.
3469, 3477, 1, 799,,,, 0., 0., 100.
*NCOPY, CHANGE NUMBER=500, OLD SET=DN700, SHIFT, NEW SET=DN800
0., 0., -0.6
0., 0., -100., 0., 0., 100., 0.
*NCOPY, CHANGE NUMBER=1000, OLD SET=DN700, SHIFT, NEW SET=DN900
0., 0., -1.2
0., 0., -100., 0., 0., 100., 0.
*NSET, NSET=CG1
3441, 3461, 3941, 3961, 4441, 4461
*NSET, NSET=CG2
3457, 3477, 3957, 3977, 4457, 4477
********** Element generation for pin **********
*ELEMENT, TYPE=DC3D8, ELSET=PEC10
1, 199, 101, 102, 111, 99, 1, 2, 11
6, 199, 111, 112, 121, 99, 11, 12, 21
11, 199, 121, 122, 131, 99, 21, 22, 31
16, 199, 131, 132, 101, 99, 31, 32, 1
```

```
*ELEMENT, TYPE=DC3D8, ELSET=PE11
2, 101, 103, 104, 102, 1,  3, 4, 2
3, 102, 104, 105, 106, 2,  4, 5, 6
4, 111, 102, 106, 113, 11, 2, 6, 13
*ELCOPY, ELEMENT SHIFT=5, OLD SET=PE11, SHIFT NODES=10, NEW SET=PE12
*ELCOPY, ELEMENT SHIFT=5, OLD SET=PE12, SHIFT NODES=10, NEW SET=PE13
*ELCOPY, ELEMENT SHIFT=5, OLD SET=PE13, SHIFT NODES=10, NEW SET=PE14
*ELEMENT, TYPE=DC3D8
19, 101, 132, 136, 103, 1, 32, 36, 3
*ELSET, ELSET=PE15
19, PEC10, PE11, PE12, PE13, PE14
*ELEMENT, TYPE=DC3D8, ELSET=PE16
21, 103, 141, 142, 104, 3, 41, 42, 4
22, 104, 142, 143, 105, 4, 42, 43, 5
23, 105, 143, 144, 106, 5, 43, 44, 6
24, 106, 144, 145, 113, 6, 44, 45, 13
25, 113, 145, 146, 114, 13, 45, 46, 14
26, 114, 146, 147, 115, 14, 46, 47, 15
27, 115, 147, 148, 116, 15, 47, 48, 16
28, 116, 148, 149, 123, 16, 48, 49, 23
29, 123, 149, 150, 124, 23, 49, 50, 24
30, 124, 150, 151, 125, 24, 50, 51, 25
31, 125, 151, 152, 126, 25, 51, 52, 26
32, 126, 152, 153, 133, 26, 52, 53, 33
33, 133, 153, 154, 134, 33, 53, 54, 34
34, 134, 154, 155, 135, 34, 54, 55, 35
35, 135, 155, 156, 136, 35, 55, 56, 36
36, 136, 156, 141, 103, 36, 56, 41, 3
*ELEMENT, TYPE=DC3D8, ELSET=PE17
41, 141, 161, 162, 142, 41, 61, 62, 42
*ELGEN, ELSET=PE18
41, 2, 20, 20, 15, 1, 1, 1
*ELEMENT, TYPE=DC3D8
56, 156, 176, 161, 141, 56, 76, 61, 41
76, 176, 196, 181, 161, 76, 96, 81, 61
*ELSET, ELSET=PE10
PE15, PE16, PE17, PE18, 56, 76
*ELCOPY, ELEMENT SHIFT=100, OLD SET=PE10, SHIFT NODES=100, NEW SET=PE20
*ELCOPY, ELEMENT SHIFT=200, OLD SET=PE10, SHIFT NODES=200, NEW SET=PE30
*ELCOPY, ELEMENT SHIFT=300, OLD SET=PE10, SHIFT NODES=300, NEW SET=PE40
*ELCOPY, ELEMENT SHIFT=400, OLD SET=PE10, SHIFT NODES=400, NEW SET=PE50
*ELCOPY, ELEMENT SHIFT=500, OLD SET=PE10, SHIFT NODES=500, NEW SET=PE60
*ELCOPY, ELEMENT SHIFT=600, OLD SET=PE10, SHIFT NODES=600, NEW SET=PE70
*ELCOPY, ELEMENT SHIFT=700, OLD SET=PE10, SHIFT NODES=700, NEW SET=PE80
*ELCOPY, ELEMENT SHIFT=800, OLD SET=PE10, SHIFT NODES=800, NEW SET=PE90
*ELEMENT, TYPE=DC3D8
```

```
681,781,2701,2702,782,681,2601,2602,682
696,796,2716,2701,781,696,2616,2601,681
*ELEMENT, TYPE=DC3D8
2601,2701,2721,2722,2702,2601,2621,2622,2602
2616,2716,2736,2721,2701,2616,2636,2621,2601
2636,2736,2756,2741,2721,2636,2656,2641,2621
*ELGEN,ELSET=PE670
681,1,,,15,1,1,1
2601,2,20,20,15,1,1,1
*ELSET,ELSET=PE60X
PE670,696,2616,2636
*ELSET, ELSET=PEALL
PE10, PE20, PE30, PE40, PE50, PE60, PE60X, PE70, PE80, PE90
*ELEMENT,TYPE=DINTER4
2701,1001,1021,1022,1002,2701,2721,2722,2702
2716,1016,1036,1021,1001,2716,2736,2721,2701
2736,1036,1056,1041,1021,2736,2756,2741,2721
*ELGEN,ELSET=PE270
2701,2,20,20,15,1,1,1
*ELSET,ELSET=PE70X
PE270,2716,2736
*ELSET, ELSET=PEX, GEN
41,56
61,76
141,156
161,176
241,256
261,276
341,356
361,376
441,456
461,476
541,556
561,576
********** Element identifiers for BC application on pin **********
*ELSET, ELSET=POUT, GEN
41, 56
141, 156
241, 256
341, 356
441, 456
541, 556
2621,2636
*ELSET, ELSET=PGOUT, GEN
761, 776
861, 876
```

```
*ELSET, ELSET=PTP01, GEN
801, 804
806, 809
811, 814
816, 819
*ELSET,ELSET=PSCT1,GEN
1,501,100
2,502,100
3,503,100
4,504,100
6,506,100
7,507,100
8,508,100
9,509,100
21,521,100
22,522,100
23,523,100
24,524,100
25,525,100
26,526,100
27,527,100
28,528,100
41,541,100
42,542,100
43,543,100
44,544,100
45,545,100
46,546,100
47,547,100
48,548,100
61,561,100
62,562,100
63,563,100
64,564,100
65,565,100
66,566,100
67,567,100
68,568,100
*ELSET,ELSET=PSCT2,GEN
601,801,100
602,802,100
603,803,100
604,804,100
606,806,100
607,807,100
608,808,100
```

609,809,100
621,821,100
622,822,100
623,823,100
624,824,100
625,825,100
626,826,100
627,827,100
628,828,100
641,841,100
642,842,100
643,843,100
644,844,100
645,845,100
646,846,100
647,847,100
648,848,100
661,861,100
662,862,100
663,863,100
664,864,100
665,865,100
666,866,100
667,867,100
668,868,100
681,688
2601,2608
2621,2628
********** Element generation for plate **********
*ELEMENT, TYPE=DC3D8
1001, 1501, 1521, 1522, 1502, 1001, 1021, 1022, 1002
*ELGEN, ELSET=AE101
1001, 15, 20, 20, 15, 1, 1, 1
*ELEMENT, TYPE=DC3D8
1016, 1516, 1536, 1521, 1501, 1016, 1036, 1021, 1001
*ELGEN, ELSET=AE116
1016, 15, 20, 20, 1,,,
*ELSET, ELSET=AE100
AE101, AE116
*ELSET, ELSET=AE101,GEN
1041,1056
1061,1076
1081,1096
1101,1116
1121,1136
1141,1156

```
1161,1176
1181,1196
1201,1216
1221,1236
1241,1256
1261,1276
1281,1296
*ELCOPY,ELEMENT    SHIFT=1000,OLD    SET=AE100,SHIFT    NODES=500,NEW
SET=AE200
*ELSET, ELSET=AEALL
AE100, AE200
********** Generaton of interface elements btn. pin and plate **********
*ELEMENT,TYPE=DINTER4
2701,1001,1021,1022,1002,2701,2721,2722,2702
2716,1016,1036,1021,1001,2716,2736,2721,2701
2736,1036,1056,1041,1021,2736,2756,2741,2721
*ELGEN,ELSET=IN270
2701,2,20,20,15,1,1,1
*ELSET,ELSET=PPINT
IN270,2716,2736
********** Element identifiers for BC application on plate **********
*ELSET, ELSET=ATP11, GEN
2001, 2016
**2021, 2036
*ELSET, ELSET=ATP12, GEN
2001, 2016
2021, 2036
2041, 2056
*ELSET, ELSET=ATP14, GEN
2021, 2036
2041, 2056
*ELSET, ELSET=ATP35, GEN
2061, 2076
2081, 2096
2101, 2116
**2121, 2136
*ELSET, ELSET=ATP15
ATP12, ATP35
*ELSET, ELSET=ATOP2, GEN
2121, 2136
2141, 2156
2161, 2176
2181, 2196
2201, 2216
2221, 2236
2241, 2256
```

```
2261, 2276
2281, 2296
*ELSET, ELSET=AEBND, GEN
1281, 1296
2281, 2296
*ELSET, ELSET=AGIN, GEN
1001, 1016
2001, 2016
*ELSET,ELSET=ASCT1,GEN
1001,1281,20
1002,1282,20
1003,1283,20
1004,1284,20
1005,1285,20
1006,1286,20
1007,1287,20
1008,1288,20
*ELSET,ELSET=ASCT2,GEN
2001,2281,20
2002,2282,20
2003,2283,20
2004,2284,20
2005,2285,20
2006,2286,20
2007,2287,20
2008,2288,20
********** Element generation for filler metal(FM Model 1) **********
** Filler metal element before melting **
*ELEMENT, TYPE=DINTER4
3021, 3021, 3041, 3042, 3022, 2001, 2021, 2022, 2002
3036, 3036,3056,3041,3021,2016,2036,2021,2001
*ELGEN, ELSET=I_ES3
3021, 3, 20, 20, 15, 1, 1, 1
*ELGEN,ELSET=I_EL3
3036,3,20,20,1
*ELSET,ELSET=I_ES
I_ES3,I_EL3
** Interface for FMC2 ****
**ELEMENT, TYPE=DINTER4
**3341,3341,3361,3362,3342,2021,2041,2042,2022
**3356,3356,3376,3361,3341,2036,2056,2041,2021
**ELGEN, ELSET=I_ESS
**3341, 1, 20, 20, 15,1,1,1
**ELSET,ELSET=I_ESX
**I_ESS,3356
**
```

```
*ELEMENT, TYPE=DC3D8
3201, 3201, 3221, 3222, 3202, 3001, 3021, 3022, 3002
3216, 3216, 3236, 3221, 3201, 3016, 3036, 3021, 3001
3221, 3221, 3241, 3242, 3222, 3021, 3041, 3042, 3022
*ELGEN, ELSET=F_EX1
3201, 4, 20, 20, 15, 1, 1, 1
*ELGEN, ELSET=F_EX2
3216, 4, 20, 20, 1, 1, 1, 1
*ELSET,ELSET=F_ES1
F_EX1,F_EX2
*ELSET, ELSET=FE1, GEN
3201, 3216
*ELSET, ELSET=FE2, GEN
3261, 3276
*ELSET,ELSET=FSCT1,GEN
3201,3208
3021,3028
3041,3048
3061,3068
3201,3208
3221,3228
3241,3248
3261,3268
*ELSET,ELSET=INTER
PPINT,I_ES
********** Element generation for filler metal (FM MODEL X) ******
** Element Generation for filler metal on stud *****
*ELEMENT, TYPE=DC3D8, ELSET=FE1X1
3101,3199, 3101, 3102, 3111, 999, 901, 902, 911
3106,3199, 3111, 3112, 3121, 999, 911, 912, 921
3111,3199, 3121, 3122, 3131, 999, 921, 922, 931
3116,3199, 3131, 3132, 3101, 999, 931, 932, 901
*ELEMENT, TYPE=DC3D8, ELSET=FE1X2
3102,3101, 3103, 3104, 3102, 901, 903, 904, 902
3103,3102, 3104, 3105, 3106, 902, 904, 905, 906
3104,3111, 3102, 3106, 3113, 911, 902, 906, 913
*ELCOPY, ELEMENT SHIFT=5, OLD SET=FE1X2, SHIFT NODES=10, NEW SET=FE1X3
*ELCOPY, ELEMENT SHIFT=5, OLD SET=FE1X3, SHIFT NODES=10, NEW SET=FE1X4
*ELCOPY, ELEMENT SHIFT=5, OLD SET=FE1X4, SHIFT NODES=10, NEW SET=FE1X5
*ELEMENT, TYPE=DC3D8
3119, 3101, 3132, 3136, 3103, 901, 932, 936, 903
*ELSET, ELSET=FE1X6
3119, FE1X1, FE1X2, FE1X3, FE1X4, FE1X5
*ELEMENT, TYPE=DC3D8, ELSET=FE1X7
3121, 3103, 3141, 3142, 3104, 903, 941, 942, 904
3122, 3104, 3142, 3143, 3105, 904, 942, 943, 905
```

```
3123, 3105, 3143, 3144, 3106, 905, 943, 944, 906
3124, 3106, 3144, 3145, 3113, 906, 944, 945, 913
3125, 3113, 3145, 3146, 3114, 913, 945, 946, 914
3126, 3114, 3146, 3147, 3115, 914, 946, 947, 915
3127, 3115, 3147, 3148, 3116, 915, 947, 948, 916
3128, 3116, 3148, 3149, 3123, 916, 948, 949, 923
3129, 3123, 3149, 3150, 3124, 923, 949, 950, 924
3130, 3124, 3150, 3151, 3125, 924, 950, 951, 925
3131, 3125, 3151, 3152, 3126, 925, 951, 952, 926
3132, 3126, 3152, 3153, 3133, 926, 952, 953, 933
3133, 3133, 3153, 3154, 3134, 933, 953, 954, 934
3134, 3134, 3154, 3155, 3135, 934, 954, 955, 935
3135, 3135, 3155, 3156, 3136, 935, 955, 956, 936
3136, 3136, 3156, 3141, 3103, 936, 956, 941, 903
*ELEMENT, TYPE=DC3D8, ELSET=FE1X8
3141, 3141, 3161, 3162, 3142, 941, 961, 962, 942
*ELGEN, ELSET=FE1X9
3141, 2, 20, 20, 15, 1, 1, 1
*ELEMENT, TYPE=DC3D8
3156, 3156, 3176, 3161, 3141, 956, 976, 961, 941
3176, 3176, 3196, 3181, 3161, 976, 996, 981, 961
*ELSET, ELSET=FMC1
FE1X6, FE1X7, FE1X8, FE1X9, 3156, 3176
*ELSET,ELSET=FSCTX,GEN
3101,3104
3106,3109
3121,3128
3141,3148
3161,3168
********** Element generation for filler metal (FM MODEL 2) ******
** Element Generation for filler metal on stud *****
*ELEMENT, TYPE=DC3D8, ELSET=FE21
5001,5599, 5501, 5502, 5511, 999, 901, 902, 911
5006,5599, 5511, 5512, 5521, 999, 911, 912, 921
5011,5599, 5521, 5522, 5531, 999, 921, 922, 931
5016,5599, 5531, 5532, 5501, 999, 931, 932, 901
*ELEMENT, TYPE=DC3D8, ELSET=FE22
5002,5501, 5503, 5504, 5502, 901, 903, 904, 902
5003,5502, 5504, 5505, 5506, 902, 904, 905, 906
5004,5511, 5502, 5506, 5513, 911, 902, 906, 913
*ELCOPY, ELEMENT SHIFT=5, OLD SET=FE22, SHIFT NODES=10, NEW SET=FE23
*ELCOPY, ELEMENT SHIFT=5, OLD SET=FE23, SHIFT NODES=10, NEW SET=FE24
*ELCOPY, ELEMENT SHIFT=5, OLD SET=FE24, SHIFT NODES=10, NEW SET=FE25
*ELEMENT, TYPE=DC3D8
5019, 5501, 5532, 5536, 5503, 901, 932, 936, 903
*ELSET, ELSET=FE26
```

5019, FE21, FE22, FE23, FE24, FE25
*ELEMENT, TYPE=DC3D8, ELSET=FE27
5021, 5503, 5541, 5542, 5504, 903, 941, 942, 904
5022, 5504, 5542, 5543, 5505, 904, 942, 943, 905
5023, 5505, 5543, 5544, 5506, 905, 943, 944, 906
5024, 5506, 5544, 5545, 5513, 906, 944, 945, 913
5025, 5513, 5545, 5546, 5514, 913, 945, 946, 914
5026, 5514, 5546, 5547, 5515, 914, 946, 947, 915
5027, 5515, 5547, 5548, 5516, 915, 947, 948, 916
5028, 5516, 5548, 5549, 5523, 916, 948, 949, 923
5029, 5523, 5549, 5550, 5524, 923, 949, 950, 924
5030, 5524, 5550, 5551, 5525, 924, 950, 951, 925
5031, 5525, 5551, 5552, 5526, 925, 951, 952, 926
5032, 5526, 5552, 5553, 5533, 926, 952, 953, 933
5033, 5533, 5553, 5554, 5534, 933, 953, 954, 934
5034, 5534, 5554, 5555, 5535, 934, 954, 955, 935
5035, 5535, 5555, 5556, 5536, 935, 955, 956, 936
5036, 5536, 5556, 5541, 5503, 936, 956, 941, 903
*ELEMENT, TYPE=DC3D8, ELSET=FE28
5041, 5541, 5561, 5562, 5542, 941, 961, 962, 942
*ELGEN, ELSET=FE29
5041, 2, 20, 20, 15, 1, 1, 1
*ELEMENT, TYPE=DC3D8
5056, 5556, 5576, 5561, 5541, 956, 976, 961, 941
5076, 5576, 5596, 5581, 5561, 976, 996, 981, 961
*ELSET, ELSET=FE20
FE26, FE27, FE28, FE29, 5056, 5076
** Element Generation for filler metal on plate *****
*ELEMENT, TYPE=DC3D8
5101, 5601, 5621, 5622, 5602, 2001,2021,2022,2002
*ELGEN, ELSET=FEA01
5101, 1, 20, 20, 15, 1, 1, 1
*ELEMENT, TYPE=DC3D8
5116, 5616, 5636, 5621, 5601,2016,2036,2021,2001
**5136, 5636, 5656, 5641, 5621, 2036, 2056, 2041, 2021
*ELSET, ELSET=FEA1,GEN
5101,5116
**ELEMENT, TYPE=DC3D8
**5121,5621,5641,5642,5622,3341,3361,3362,3342
**5136,5636,5656,5641,5621,3356,3376,3361,3341
**ELGEN, ELSET=FEA1Y
**5121, 1, 20, 20, 15,1,1,1
**ELSET, ELSET=FEA2,GEN
**5121,5136
Elements between stud and plate ***
*ELEMENT, TYPE=DC3D8, ELSET=FAP02

```
5081, 5581, 5601, 5602, 5582, 981, 2001, 2002, 982
5082, 5582, 5602, 5603, 5583, 982, 2002, 2003, 983
5083, 5583, 5603, 5604, 5584, 983, 2003, 2004, 984
5084, 5584, 5604, 5605, 5585, 984, 2004, 2005, 985
5085, 5585, 5605, 5606, 5586, 985, 2005, 2006, 986
5086, 5586, 5606, 5607, 5587, 986, 2006, 2007, 987
5087, 5587, 5607, 5608, 5588, 987, 2007, 2008, 988
5088, 5588, 5608, 5609, 5589, 988, 2008, 2009, 989
5089, 5589, 5609, 5610, 5590, 989, 2009, 2010, 990
5090, 5590, 5610, 5611, 5591, 990, 2010, 2011, 991
5091, 5591, 5611, 5612, 5592, 991, 2011, 2012, 992
5092, 5592, 5612, 5613, 5593, 992, 2012, 2013, 993
5093, 5593, 5613, 5614, 5594, 993, 2013, 2014, 994
5094, 5594, 5614, 5615, 5595, 994, 2014, 2015, 995
5095, 5595, 5615, 5616, 5596, 995, 2015, 2016, 996
5096, 5596, 5616, 5601, 5581, 996, 2016, 2001, 981
*ELSET,ELSET=FMC2
FE20,FEA1,FAP02
*ELSET,ELSET=FSCT2,GEN
5001,5004
5006,5009
5021,5028
5041,5048
5061,5068
5081,5088
5101,5108
5121,5128
5141,5148
5301,5308
5381,5388
********** Element generation for filler metal (FM MODEL 3) ******
*ELEMENT, TYPE=DC3D8, ELSET=FE31
6001,6599, 6501, 6502, 6511, 999, 901, 902, 911
6006,6599, 6511, 6512, 6521, 999, 911, 912, 921
6011,6599, 6521, 6522, 6531, 999, 921, 922, 931
6016,6599, 6531, 6532, 6501, 999, 931, 932, 901
*ELEMENT, TYPE=DC3D8, ELSET=FE32
6002,6501, 6503, 6504, 6502, 901, 903, 904, 902
6003,6502, 6504, 6505, 6506, 902, 904, 905, 906
6004,6511, 6502, 6506, 6513, 911, 902, 906, 913
*ELCOPY, ELEMENT SHIFT=5, OLD SET=FE32, SHIFT NODES=10, NEW SET=FE33
*ELCOPY, ELEMENT SHIFT=5, OLD SET=FE33, SHIFT NODES=10, NEW SET=FE34
*ELCOPY, ELEMENT SHIFT=5, OLD SET=FE34, SHIFT NODES=10, NEW SET=FE35
*ELEMENT, TYPE=DC3D8
6019, 6501, 6532, 6536, 6503, 901, 932, 936, 903
*ELSET, ELSET=FE36
```

```
6019, FE31, FE32, FE33, FE34, FE35
*ELEMENT, TYPE=DC3D8, ELSET=FE37
6021, 6503, 6541, 6542, 6504, 903, 941, 942, 904
6022, 6504, 6542, 6543, 6505, 904, 942, 943, 905
6023, 6505, 6543, 6544, 6506, 905, 943, 944, 906
6024, 6506, 6544, 6545, 6513, 906, 944, 945, 913
6025, 6513, 6545, 6546, 6514, 913, 945, 946, 914
6026, 6514, 6546, 6547, 6515, 914, 946, 947, 915
6027, 6515, 6547, 6548, 6516, 915, 947, 948, 916
6028, 6516, 6548, 6549, 6523, 916, 948, 949, 923
6029, 6523, 6549, 6550, 6524, 923, 949, 950, 924
6030, 6524, 6550, 6551, 6525, 924, 950, 951, 925
6031, 6525, 6551, 6552, 6526, 925, 951, 952, 926
6032, 6526, 6552, 6553, 6533, 926, 952, 953, 933
6033, 6533, 6553, 6554, 6534, 933, 953, 954, 934
6034, 6534, 6554, 6555, 6535, 934, 954, 955, 935
6035, 6535, 6555, 6556, 6536, 935, 955, 956, 936
6036, 6536, 6556, 6541, 6503, 936, 956, 941, 903
*ELEMENT, TYPE=DC3D8, ELSET=FE38
6041, 6541, 6561, 6562, 6542, 941, 961, 962, 942
*ELGEN, ELSET=FE39
6041, 2, 20, 20, 15, 1, 1, 1
*ELEMENT, TYPE=DC3D8
6056, 6556, 6576, 6561, 6541, 956, 976, 961, 941
6076, 6576, 6596, 6581, 6561, 976, 996, 981, 961
*ELSET, ELSET=FE30
FE36, FE37, FE38, FE39, 6056, 6076
** Element Generation for filler metal on plate *****
*ELEMENT, TYPE=DC3D8
6101, 6601, 6621, 6622, 6602, 2001, 2021, 2022, 2002
*ELGEN, ELSET=FEA02
6101, 2, 20, 20, 16, 1, 1, 1
*ELEMENT, TYPE=DC3D8
6116, 6616, 6636, 6621, 6601, 2016, 2036, 2021, 2001
6136, 6636, 6656, 6641, 6621, 2036, 2056, 2041, 2021
*ELSET, ELSET=FEA30
FEA02, 6116, 6136
**
*ELEMENT, TYPE=DC3D8, ELSET=FAP03
6081, 6581, 6601, 6602, 6582, 981, 2001, 2002, 982
6082, 6582, 6602, 6603, 6583, 982, 2002, 2003, 983
6083, 6583, 6603, 6604, 6584, 983, 2003, 2004, 984
6084, 6584, 6604, 6605, 6585, 984, 2004, 2005, 985
6085, 6585, 6605, 6606, 6586, 985, 2005, 2006, 986
6086, 6586, 6606, 6607, 6587, 986, 2006, 2007, 987
6087, 6587, 6607, 6608, 6588, 987, 2007, 2008, 988
```

```
6088, 6588, 6608, 6609, 6589, 988, 2008, 2009, 989
6089, 6589, 6609, 6610, 6590, 989, 2009, 2010, 990
6090, 6590, 6610, 6611, 6591, 990, 2010, 2011, 991
6091, 6591, 6611, 6612, 6592, 991, 2011, 2012, 992
6092, 6592, 6612, 6613, 6593, 992, 2012, 2013, 993
6093, 6593, 6613, 6614, 6594, 993, 2013, 2014, 994
6094, 6594, 6614, 6615, 6595, 994, 2014, 2015, 995
6095, 6595, 6615, 6616, 6596, 995, 2015, 2016, 996
6096, 6596, 6616, 6601, 6581, 996, 2016, 2001, 981
**
*ELEMENT, TYPE=DC3D6
6641,6641,2041,2061,6642,2042,2062
6656,6656,2056,2076,6641,2041,2061
*ELGEN, ELSET=FE30X
6641, 1, , , 15, 1, 1, 1
*ELSET,ELSET=FE3D6
FE30X,6656
*ELSET,ELSET=FMC3
FE30,FEA30,FAP03,FE3D6
*ELSET,ELSET=F_ES
F_ES1,FMC1,FMC2,FMC3
*ELSET,ELSET=FSCT3,GEN
6001,6004
6006,6009
6021,6028
6041,6048
6061,6068
6081,6088
6101,6108
6121,6128
6641,6648
** Element generation for braze gap ******
*ELEMENT, TYPE=DC3D8, ELSET=GE01
781, 881, 1501, 1502, 882, 781, 1001, 1002, 782
782, 882, 1502, 1503, 883, 782, 1002, 1003, 783
783, 883, 1503, 1504, 884, 783, 1003, 1004, 784
784, 884, 1504, 1505, 885, 784, 1004, 1005, 785
785, 885, 1505, 1506, 886, 785, 1005, 1006, 786
786, 886, 1506, 1507, 887, 786, 1006, 1007, 787
787, 887, 1507, 1508, 888, 787, 1007, 1008, 788
788, 888, 1508, 1509, 889, 788, 1008, 1009, 789
789, 889, 1509, 1510, 890, 789, 1009, 1010, 790
790, 890, 1510, 1511, 891, 790, 1010, 1011, 791
791, 891, 1511, 1512, 892, 791, 1011, 1012, 792
792, 892, 1512, 1513, 893, 792, 1012, 1013, 793
793, 893, 1513, 1514, 894, 793, 1013, 1014, 794
```

794, 894, 1514, 1515, 895, 794, 1014, 1015, 795
795, 895, 1515, 1516, 896, 795, 1015, 1016, 796
796, 896, 1516, 1501, 881, 796, 1016, 1001, 781
**
*ELEMENT, TYPE=DC3D8, ELSET=GE02
881, 981, 2001, 2002, 982, 881, 1501, 1502, 882
882, 982, 2002, 2003, 983, 882, 1502, 1503, 883
883, 983, 2003, 2004, 984, 883, 1503, 1504, 884
884, 984, 2004, 2005, 985, 884, 1504, 1505, 885
885, 985, 2005, 2006, 986, 885, 1505, 1506, 886
886, 986, 2006, 2007, 987, 886, 1506, 1507, 887
887, 987, 2007, 2008, 988, 887, 1507, 1508, 888
888, 988, 2008, 2009, 989, 888, 1508, 1509, 889
889, 989, 2009, 2010, 990, 889, 1509, 1510, 890
890, 990, 2010, 2011, 991, 890, 1510, 1511, 891
891, 991, 2011, 2012, 992, 891, 1511, 1512, 892
892, 992, 2012, 2013, 993, 892, 1512, 1513, 893
893, 993, 2013, 2014, 994, 893, 1513, 1514, 894
894, 994, 2014, 2015, 995, 894, 1514, 1515, 895
895, 995, 2015, 2016, 996, 895, 1515, 1516, 896
896, 996, 2016, 2001, 981, 896, 1516, 1501, 881
*ELSET, ELSET=G_ES
GE01, GE02
*ELSET,ELSET=GSCT1,GEN
781,788
881,888
*ELSET, ELSET=HSCT
ASCT1,ASCT2,PSCT1,PSCT2,FSCT1,FSCT2,FSCT3,GSCT1
*ELSET, ELSET=HSCT1
ASCT1,ASCT2,PSCT2,FSCT1,FSCT2,FSCT3,GSCT1
********** Element identifier for heat flux application **********
*ELSET, ELSET=LFLUX
PE90,F_ES1,ATP35
**PE90, F_ES1, ATP14,ATP35
********** Application multi-point constraints **********
*MPC
**TIE, CA101, CA102
**TIE, CA151, CA152
**TIE, CA201, CA202
TIE, CP01, CP02
**TIE, CF11, CF12
**TIE, CF21, CF22
TIE, CG1, CG2
********** Thermal properties for materials **********
*SOLID SECTION, ELSET=PEALL, MATERIAL=AISI304
*MATERIAL,NAME=AISI304

*SPECIFIC HEAT
0.3350, 27.
0.3568, 127.
0.3939, 327.
0.4245, 527.
0.4446, 727.
0.4559, 927.
*DENSITY
8.03E-3, 27.
7.98E-3, 127.
7.89E-3, 327.
7.80E-3, 527.
7.71E-3, 727.
7.62E-3, 927.
*CONDUCTIVITY
1.329E-2, 27.
1.541E-2, 127.
1.917E-2, 327.
2.294E-2, 527.
2.635E-2, 727.
3.012E-2, 927.
*SOLID SECTION, ELSET=AEALL, MATERIAL=AL5052
*MATERIAL, NAME=AL5052
*SPECIFIC HEAT
0.8875,20.
0.9185,76.8
0.9317,126.8
0.9783,226.8
1.0258,336.8
1.0774,446.8
1.131,526.8
1.2033,607.
1.0897,649.
1.0897,1093.3
*DENSITY
2.670E-3, 20.
2.669E-3, 93.3
2.644E-3, 204.4
2.608E-3, 315.6
2.587E-3, 426.7
2.554E-3, 537.8
2.521E-3, 649.0
2.360E-3, 654.0
2.343E-3, 760.
2.316E-3, 871.1
2.285E-3, 982.2

2.248E-3, 1093.3
*CONDUCTIVITY
0.236, 20.
0.238, 93.3
0.238, 204.4
0.232, 315.6
0.223, 426.7
0.216, 537.8
0.205, 649.0
0.09, 654.0
0.100, 1093.3
*LATENT HEAT
408., 607., 649.
*SOLID SECTION, ELSET=F_ES, MATERIAL=AL12SI
*MATERIAL,NAME=AL12SI
*SPECIFIC HEAT
0.8875,20.
0.9185,76.8
0.9317,126.8
0.9783,226.8
1.0258,336.8
1.0774,446.8
1.131,526.8
1.1723,577.
1.0897,582.
1.0897,1093.3
*DENSITY
2.664E-3, 20.
2.653E-3, 93.3
2.628E-3, 204.4
2.593E-3, 315.6
2.572E-3, 426.7
2.516E-3, 582.
2.378E-3, 587.
2.346E-3, 660.
2.302E-3, 760.
2.276E-3, 871.1
2.245E-3, 982.2
2.234E-3, 1093.3
*CONDUCTIVITY
0.236, 20.
0.238, 93.3
0.238, 204.4
0.232, 315.6
0.223, 426.7
0.216, 537.8

0.212, 582.
0.085, 587.
0.100, 1093.3
*LATENT HEAT
540.000, 577., 582.
*SOLID SECTION, ELSET=G_ES, MATERIAL=AL12%SI
*MATERIAL,NAME=AL12%SI
*SPECIFIC HEAT
0.8875,20.
0.9185,76.8
0.9317,126.8
0.9783,226.8
1.0258,336.8
1.0774,446.8
1.131,526.8
1.1723,577.
1.0897,582.
1.0897,1093.3
**
*DENSITY
2.664E-3, 20.
2.653E-3, 93.3
2.628E-3, 204.4
2.593E-3, 315.6
2.572E-3, 426.7
2.516E-3, 582.
2.378E-3, 587.
2.346E-3, 660.
2.302E-3, 760.
2.276E-3, 871.1
2.245E-3, 982.2
2.234E-3, 1093.3
*CONDUCTIVITY
0.236, 20.
0.238, 93.3
0.238, 204.4
0.232, 315.6
0.223, 426.7
0.216, 537.8
0.212, 582.
0.085, 587.
0.100, 1093.3
*LATENT HEAT
540.000, 577., 582.
*PHYSICAL CONSTANTS,ABSOLUTE ZERO=-273.16
********** Apply thermal interface conditions for filler metal **********

```
*INTERFACE,ELSET=INTER
*GAP CONDUCTANCE, DEPENDENCIES=1
0., 3.5E-5
**GAP RADIATION
**0.486E-15, 0.486E-15, -273.16
********** Provide initial conditions(TEMP. DEG. C) **********
*INITIAL CONDITIONS, TYPE=TEMPERATURE
PNALL, 20.
ANALL, 20.
FNALL, 20.
FBND1, 20.
FBND2, 20.
FBND3, 20.
999, 20.
**
*AMPLITUDE, NAME=GFILL
0., 0., 0.0001, 1.
*AMPLITUDE, NAME=GBND
0., 0., 0.0001, 1.
*RESTART, WRITE, FREQ=999
********** Step 1: Heating cycle upto the filler metal's melting ******
*STEP, INC=50000,UNSYMM=YES
STEP 1
*HEAT TRANSFER, DELTMX=200., END=PERIOD
3.3E-2, .84
**CONTROLS, ANALYSIS=DISCONTINUOUS
**CONTROLS, PARAMETERS=TIME INCREMENTATION
**8, 10
*CONTROLS, PARAMETERS=FIELD, FIELD=TEMPERATURE
5.E-2, 1.E-1,,, 1.E-1
*MODEL CHANGE, REMOVE
PEX,G_ES,FMC1,FMC2,FMC3
********** Apply heat loss from the surfaces **********
*FILM
**FE1, F2, 20., 10.E-6
**FE1, F6, 20., 10.E-6
**FE2, F4, 20., 10.E-6
**F_ES1, F1, 20., 10.E-6
PGOUT, F4, 20., 10.E-6
POUT, F4, 20., 10.E-6
PE10, F2, 20., 10.E-6
**PE90, F1, 20., 10.E-6
PE60X, F2, 20., 10.E-6
**ATP35, F1, 20., 10.E-6
ATOP2, F1, 20., 10.E-6
AE101, F2, 20., 10.E-6
```

```
AEBND, F4, 20., 10.E-6
AGIN, F6, 20., 10.E-6
*RADIATE
**FE1, R2, 20., 0.486E-15
**FE1, R6, 20., 0.486E-15
**FE2, R4, 20., 0.486E-15
**F_ES1, R1, 20., 0.486E-15
PGOUT, R4, 20., 1.35E-15
POUT, R4, 20, 1.35E-15
PE10, R2, 20., 1.35E-15
**PE90, R1, 20., 1.35E-15
PE60X, R2, 20., 1.35E-15
**ATP35, R1, 20., 0.486E-15
ATOP2, R1, 20., 0.486E-15
AE101, R2, 20., 0.486E-15
AEBND, R4, 20., 0.486E-15
AGIN, R6, 20., 0.486E-15
********** Apply heat flux from by laser beam **********
*DFLUX
LFLUX, S1NU
*USER SUBROUTINES
    SUBROUTINE DFLUX (FLUX,TEMP,KSTEP,KINC,TIME,NOEL,NPT,COORDS,JLTYP)
C
    INCLUDE 'ABA_PARAM.INC'
C
    DIMENSION FLUX(2),TIME(2),COORDS(3)
C
    POWER=600.
    ABSORP=0.1
    EFFRAD=3.75
    PHI=3.141592
C
    IF(TIME(2).GE.0.4) ABSORP=0.35
C     IF(KSTEP.GE.2) ABSORP=0.35
    IF(NOEL.LT.3000)GO TO 100
      IF(TEMP.GT.577.AND.TEMP.LE.582.) ABSORP=0.5
      IF(TEMP.GT.582.AND.TEMP.LE.800.) ABSORP=0.69
      IF(TEMP.GT.800.AND.TEMP.LE.1200.) ABSORP=0.79
C
C     IF(TEMP.GT.1000.AND.TEMP.LE.1200.) ABSORP=0.6
C     IF(TEMP.GT.1200.AND.TEMP.LE.1500.) ABSORP=0.7
C
 100 APOWER=0.63*ABSORP*POWER
    ERSQ=EFFRAD**2.
    RAD=(COORDS(1)**2.+COORDS(2)**2.)**0.5
    RSHIFT=(EFFRAD/2.)-0.5
```

```
    RERSQ=((RAD-RSHIFT)/(EFFRAD/2.))**2.
    FLUX(1)=((3.*APOWER)/(PHI*ERSQ))*EXP(-3.*RERSQ)
    FLUX(2)=0.
    RETURN
    END
**
********** Print nodal temperature and save results in file **********
*RESTART, WRITE, FREQ=10
*NODE PRINT, FREQ=2, NSET=CF11
NT
*NODE PRINT, FREQ=2, NSET=CF21
NT
*NODE PRINT, FREQ=2, NSET=CA200
NT
*NODE PRINT, FREQ=2, NSET=GANS
NT
*NODE PRINT, FREQ=2, NSET=GPNS
NT
*NODE PRINT, FREQ=2, NSET=PN90
NT
*NODE FILE, FREQ=2
NT
*END STEP
********** Step: Heating after model change 1 ****
****** Step 2: Intermediate step to apply BC for model change 2 ****
*STEP, INC=5000,UNSYMM=YES
STEP 2
*HEAT TRANSFER, DELTMX=700., END=PERIOD
3.3E-2, 0.0001
**CONTROLS, ANALYSIS=DISCONTINUOUS
*CONTROLS, PARAMETERS=FIELD, FIELD=TEMPERATURE
5.E-2, 1.E-1,,, 1.E-1
*MODEL CHANGE, REMOVE
I_ES,F_ES1
*MODEL CHANGE, ADD
FMC2
*BOUNDARY
FBND2,11,, 857.
PN90, 11,, 827.
**FBNDX, 11,, 920.
**AAP02,11,, 920.
AX901,11,,827.
AX902,11,,827.
**AX903,11,,920
********** Apply additional heat loss from the surfaces **********
*FILM
```

```
POUT, F4, 20., 10.E-6
PE10, F2, 20., 10.E-6
PE60X, F2, 20., 10.E-6
**FMC2, F1, 20., 10.E-6
**FEA1, F4, 20., 10.E-6
**ATP14, F1, 20., 10.E-6
**ATP35, F1, 20., 10.E-6
ATOP2, F1, 20., 10.E-6
AE101, F2, 20., 10.E-6
AEBND, F4, 20., 10.E-6
**GE01, F2, 20., 10.E-6
**GE02, F1, 20., 10.E-6
*RADIATE
POUT, R4, 20., 1.35E-15
PE10, R2, 20., 1.35E-15
PE60X, R2, 20., 1.35E-15
**FMC2, R1, 20., 0.486E-15
**FEA1, R4, 20., 0.486E-15
**ATP14, R1, 20., 0.486E-15
**ATP35, R1, 20., 0.486E-15
ATOP2, R1, 20., 0.486E-15
AE101, R2, 20., 0.486E-15
AEBND, R4, 20., 0.486E-15
**GE01, R2, 20., 0.486E-15
**GE02, R1, 20., 0.486E-15
*DFLUX
FMC2, S1NU
ATP14,S1NU
ATP35, S1NU
*****Print nodal temperature and save results in file **********
*RESTART, WRITE, FREQ=10
*NODE PRINT, FREQ=2, NSET=CA200
NT
*NODE PRINT, FREQ=2, NSET=GANS
NT
*NODE PRINT, FREQ=2, NSET=GPNS
NT
*NODE PRINT, FREQ=2, NSET=FBND2
NT
*NODE PRINT, FREQ=2, NSET=PN90
NT
*NODE FILE, FREQ=2
NT
*END STEP
********** Step 3: Heating after the model change 2 ****
*STEP, INC=50000,UNSYMM=YES
```

```
STEP 3
*HEAT TRANSFER, DELTMX=1000., END=PERIOD
3.3E-2, 2.365
**CONTROLS, ANALYSIS=DISCONTINUOUS
*CONTROLS, PARAMETERS=FIELD, FIELD=TEMPERATURE
5.E-2, 1.E-1,,, 1.E-1
*BOUNDARY, OP=NEW
********** Apply additional heat loss from the surfaces **********
*FILM
POUT, F4, 20., 10.E-6
PE10, F2, 20., 10.E-6
PE60X, F2, 20., 10.E-6
**FMC2, F1, 20., 10.E-6
**FEA1, F4, 20., 10.E-6
**ATP14, F1, 20., 10.E-6
**ATP35, F1, 20., 10.E-6
ATOP2, F1, 20., 10.E-6
AE101, F2, 20., 10.E-6
AEBND, F4, 20., 10.E-6
GE01, F2, 20., 10.E-6
GE02, F1, 20., 10.E-6
*RADIATE
POUT, R4, 20., 1.35E-15
PE10, R2, 20., 1.35E-15
PE60X, R2, 20., 1.35E-15
**FMC2, R1, 20., 0.486E-15
**FEA1, R4, 20., 0.486E-15
**ATP14, R1, 20., 0.486E-15
**ATP35, R1, 20., 0.486E-15
ATOP2, R1, 20., 0.486E-15
AE101, R2, 20., 0.486E-15
AEBND, R4, 20., 0.486E-15
GE01, R2, 20., 0.486E-15
GE02, R1, 20., 0.486E-15
*DFLUX
FMC2, S1NU
ATP14,S1NU
ATP35, S1NU
*****Print nodal temperature and save results in file **********
*RESTART, WRITE, FREQ=10
*NODE PRINT, FREQ=2, NSET=CA200
NT
*NODE PRINT, FREQ=2, NSET=GANS
NT
*NODE PRINT, FREQ=2, NSET=GPNS
NT
```

```
*NODE PRINT, FREQ=2, NSET=FBND2
NT
*NODE PRINT, FREQ=2, NSET=PN90
NT
*NODE FILE, FREQ=2
NT
*END STEP
********** Step 4: Intermediate step for model change 3 ****
*STEP, INC=5000,UNSYMM=YES
STEP 4
*HEAT TRANSFER, DELTMX=750., END=PERIOD
3.3E-2, 0.0001
**CONTROLS, ANALYSIS=DISCONTINUOUS
*CONTROLS, PARAMETERS=FIELD, FIELD=TEMPERATURE
5.E-2, 1.E-1,,, 1.E-1
*MODEL CHANGE, REMOVE
FMC2
*MODEL CHANGE, ADD
FMC3,G_ES
*BOUNDARY
FBND3, 11,,785.
PN90, 11,, 785.
GPNS, 11,, 785.
GANS, 11,, 785.
********** Apply additional heat loss from the surfaces **********
*FILM
POUT, F4, 20., 10.E-6
PE10, F2, 20., 10.E-6
PE60X, F2, 20., 10.E-6
**FMC3, F1, 20., 10.E-6
**ATP35, F1, 20., 10.E-6
ATOP2, F1, 20., 10.E-6
AE101, F2, 20., 10.E-6
AEBND, F4, 20., 10.E-6
*RADIATE
POUT, R4, 20., 1.35E-15
PE10, R2, 20., 1.35E-15
PE60X, R2, 20., 1.35E-15
**FMC3, R1, 20., 0.486E-15
**ATP35, R1, 20., 0.486E-15
ATOP2, R1, 20., 0.486E-15
AE101, R2, 20., 0.486E-15
AEBND, R4, 20., 0.486E-15
*DFLUX
FMC3, S1NU
FE3D6, S5NU
```

```
ATP35, S1NU
*****Print nodal temperature and save results in file **********
*RESTART, WRITE, FREQ=10
*NODE PRINT, FREQ=2, NSET=FBND3
NT
*NODE PRINT, FREQ=2, NSET=CA200
NT
*NODE PRINT, FREQ=2, NSET=GANS
NT
*NODE PRINT, FREQ=2, NSET=GPNS
NT
*NODE PRINT, FREQ=2, NSET=PN90
NT
*NODE FILE, FREQ=2
NT
*END STEP
********** Step 5: Heating cycle after model change 3 **********
*STEP, INC=500000,UNSYMM=YES
STEP 5
*HEAT TRANSFER, DELTMX=1000., END=PERIOD
3.3E-2, 0.2
*BOUNDARY, OP=NEW
********** Apply additional heat loss from the surfaces **********
*FILM
POUT, F4, 20., 10.E-6
PE10, F2, 20., 10.E-6
PE60X, F2, 20., 10.E-6
**FMC3, F1, 20., 10.E-6
**ATP35, F1, 20., 10.E-6
ATOP2, F1, 20., 10.E-6
AE101, F2, 20., 10.E-6
AEBND, F4, 20., 10.E-6
*RADIATE
POUT, R4, 20., 1.35E-15
PE10, R2, 20., 1.35E-15
PE60X, R2, 20., 1.35E-15
**FMC3, R1, 20., 0.486E-15
**ATP35, R1, 20., 0.486E-15
ATOP2, R1, 20., 0.486E-15
AE101, R2, 20., 0.486E-15
AEBND, R4, 20., 0.486E-15
*DFLUX
FMC3, S1NU
FE3D6, S5NU
ATP35, S1NU
*****Print nodal temperature and save results in file **********
```

```
*RESTART, WRITE, FREQ=10
*NODE PRINT, FREQ=2, NSET=FBND3
NT
*NODE PRINT, FREQ=2, NSET=CA200
NT
*NODE PRINT, FREQ=2, NSET=GANS
NT
*NODE PRINT, FREQ=2, NSET=GPNS
NT
*NODE PRINT, FREQ=2, NSET=PN90
NT
*NODE FILE, FREQ=2
NT
*END STEP
********** Step 6: Cooling cycle after beam on time **********
*STEP, INC=500000,UNSYMM=YES
STEP 6
*HEAT TRANSFER, DELTMX=300., END=PERIOD
3.3E-2, 7.
*CONTROLS, RESET
********** Apply additional heat loss from the surfaces **********
*FILM
POUT, F4, 20., 10.E-6
PE10, F2, 20., 10.E-6
PE60X, F2, 20., 10.E-6
**FMC3, F1, 20., 10.E-6
**ATP35, F1, 20., 10.E-6
ATOP2, F1, 20., 10.E-6
AE101, F2, 20., 10.E-6
AEBND, F4, 20., 10.E-6
*RADIATE
POUT, R4, 20., 1.35E-15
PE10, R2, 20., 1.35E-15
PE60X, R2, 20., 1.35E-15
**FMC3, R1, 20., 0.486E-15
**ATP35, R1, 20., 0.486E-15
ATOP2, R1, 20., 0.486E-15
AE101, R2, 20., 0.486E-15
AEBND, R4, 20., 0.486E-15
*DFLUX, OP=NEW
*****Print nodal temperature and save results in file **********
*RESTART, WRITE, FREQ=10
*NODE PRINT, FREQ=2, NSET=FBND3
NT
*NODE PRINT, FREQ=2, NSET=CA200
NT
```

```
*NODE PRINT, FREQ=2, NSET=GANS
NT
*NODE PRINT, FREQ=2, NSET=GPNS
NT
*NODE PRINT, FREQ=2, NSET=PN90
NT
*NODE FILE, FREQ=2
NT
*END STEP
```

서 지 정 보 양 식			
수행기관보고서번호	위탁기관보고서번호	표준보고서번호	INIS주제코드
KAERI/TR-693/96			

제목/부제	이종금속 스터드와 평판간 레이저 브래이징 접합부의 열해석을 위한 유한요소 모델링

연구책임자 및 부서명 (TR, AR은 주저자명)	박준수(계통기계분야)
연구자 및 부서명	김종민(계통기계분야)

발 행 지	대 전	발행기관	한국원자력연구소	발 행 일	1996. 6.
페 이 지	62 P.	도 표	유(V), 무( )	크 기	26 Cm.
참고사항					

비밀여부	공개(V), 대외비( ), _급비밀	보고서종류	기술보고서
연구위탁기관		계약 번호	

초록 (300단어 내외)

본 연구를 통하여 스터드와 평판간 레이저 브래이징의 열전달 해석을 위한 유한요소모델을 개발하였으며, 3차원 유한요소모델을 통하여 과도 온도장을 해석하였다. 근사적인 수치해를 구하기 위하여 ABAQUS 유한요소 프로그램 및 사용자 서브루틴을 사용하였다. 해석시 온도에 따라 변하는 열적 물성치, 잠열의 효과, 대류 및 복사에 의한 열손실을 고려하였다. 브래이징 재료는 AISI304 스테인레스강 스터드와 A15052 평판이며 88Al-12Si 브래이징 합금을 용가재로 사용하였다. 열원으로서 준(pseudo) TM_{01*}모드의 연속파 CO_2 레이저를 사용하였으며, 이를 위하여 발진기에 의해 발생되는 TM_{00}모드의 레이저빔(laser beam)을 엑시콘랜즈(axicon lens)를 사용하여 광학적으로 변조하였다. 한편, 고속운동분석기(high speed motion analyser)를 사용하여 브래이징시 용가재의 젖음(wetting) 및 퍼짐(spreading)을 포함한 용가재의 이동을 관찰하였으며, 이의 결과를 토대로 하여 유한요소모델링시 해의 영역과 경계조건을 정의하였다. 수학적 모델의 검증을 위해 전형적인 공정파라메타에 대한 수치해를 구하고, 이 결과를 적외선 및 열전대를 이용한 온도측정 및 실험결과와 비교하였다.

주제명 키워드 (10단어 내외)

브래이징, CO_2 레이저, $TM01^*$ 모드, 표면장력, 모세관 현상, 알루미늄 A15052, 스텐레스강 AISI304, 유한요소법

BIBLIOGRAPHIC INFORMATION SHEET			
Performing Org. Report No.	Sponsoring Org. Report No.	Standard Report No.	INIS Subject Code
KAERI/TR-693/96			

Title/Subtitle	Finite element modelling for thermal analysis of stud-to-plate laser brazing for a dissimilar metal joint
Project Manager and Dep	Park, June-Soo(Systems Mechanical Design Dept.)
Researcher and Dept	Kim, Jong-Min(Systems Mechanical Design Dept.)

Pub. Place	Daejeon	Pub. Org	KAERI	Pub. Date	1996. 6.
Page	62 P.	Fig. and Tab.	Yes(o), No( )	Size	26 Cm.
Note					

Classified	Open(o), Outside( ), _ Class	Report Type	Technical Report
Sponsoring Org.		Contract No.	

Abstract (about 300 Words)

A finite element model was developed for the thermal analisis of a stud-to-plate laser brazing joint, and the transient temperature fields were analysed by using a three-dimensional model. The finite element program ABAQUS, together with a few user subroutines, was employed to perform the numerical approximation. Temperature-dependent thermal properties, effect of latent heat, and the convection and radiative heat losses were considered. The brazing parts used were AISI 304 stainless steel stud and aluminium Al 5052 plate, and the brazing alloy 88Al-12Si was used as filler metal. A pseudo-TM_{01}^{*} mode of the cw CO_2 laser beam was used as heat source, for which TM_{00} mode generated by beam oscillator was optically modulated using axicon lens. Re-location of the filler metal during the brazing process including its wetting and spreading was examined by using a high speed motion analyser, and the results were incorporated in the FEM modelling for defining the solution domain and boundary conditions. The numerical results were obtained for typical process parameters, and were compoared with experimental ones determined by using the infrared and thermocouple measurements.

Subject Keywords (about 10 words)

Brazing, CO_2 laser, TM_{01}^{*} Mode, Surface tension, Capillarity, Aluminium Al5052, Stainless Steel AISI304, Finite Element Method